Highly Potent and Selective Histone Deacetylase 6 Inhibitors Designed Based on a Small-Molecular Substrate

Takayoshi Suzuki,*,† Akiyasu Kouketsu,† Yukihiro Itoh,† Shinya Hisakawa,† Satoko Maeda,‡ Minoru Yoshida,‡,§ Hidehiko Nakagawa,† and Naoki Miyata*,†

Graduate School of Pharmaceutical Sciences, Nagoya City University, 3-1 Tanabe-dori, Mizuho-ku, Nagoya, Aichi 467-8603, Japan, RIKEN, Saitama 351-0198, Japan, and CREST Research Project, Japan Science and Technology Agency, Saitama 332-001, Japan

Received May 11, 2006

Abstract: To find novel histone deacetylase 6 (HDAC6)-selective inhibitors and clarify the structural requirements for HDAC6-selective inhibition, we prepared thiolate analogues designed based on the structure of an HDAC6-selective substrate and evaluated the histone/α-tubulin acetylation selectivity by Western blot analysis. Aliphatic compounds **17b**–**20b** selectively caused α-tubulin acetylation over histone H4 acetylation. In enzyme assays using HDAC1, HDAC4, and HDAC6, compounds **17a**–**19a** exhibited HDAC6-selective inhibition over HDAC1 and HDAC4.

Introduction

Histone deacetylases[a] (HDACs) are responsible for the deacetylation of the acetylated lysine residues in the N-terminal region of the core histones and are involved in transcriptional regulation, cell cycle progression, and developmental events.[1] Thus far, eighteen HDAC family members have been identified, and they are divided into two categories, i.e., zinc-dependent enzymes (HDAC1–11) and NAD^+-dependent enzymes (SIRT1–7).[1a,2] HDAC6, a zinc-dependent HDAC isoform, is unique in that it is cytoplasmic and participates in the deacetylation of nonhistone proteins, such as α-tubulin and HSP90, as well as regulating important biological processes including microtubule stability and function, and molecular chaperon activity.[3] In addition, it has recently been reported that inhibition of HDAC6 has an antitumor effect in multiple myeloma cells.[4] Thus, HDAC6-selective inhibitors are of interest not only as tools for elucidating the more intricate biological functions of HDAC6, but also as candidate antitumor agents.

A number of structurally diverse HDAC inhibitors have been identified,[5] including **1** (trichostatin A, TSA),[6] **2** (suberoylanilide hydroxamic acid, SAHA),[7] **3** (CHAP31),[8] **4** (trapoxin B, TPX B),[6h,9] and **5** (MS-275)[10] (Chart 1). Most hydroxamates, such as **1** and **2**, inhibit all of the HDAC isoforms, whereas most non-hydroxamates, such as **4** and **5**, do not inhibit HDAC6.[3b,c,11] To date, the only known HDAC6-selective inhibitor is **6** (tubacin) (Chart 1), which was discovered using a combinatorial approach.[12] At present, there is little information about the structural requirements for HDAC6-selective inhibition. Therefore, there is a need to develop novel HDAC6-selective inhibitors and then to study their structure–activity relationships.

Chart 1. Examples of HDAC Inhibitors

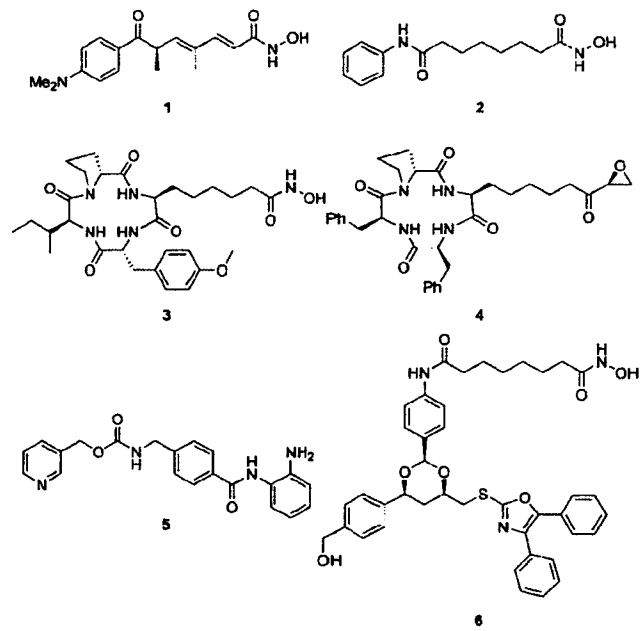

Chart 2. Thiolate HDAC Inhibitors

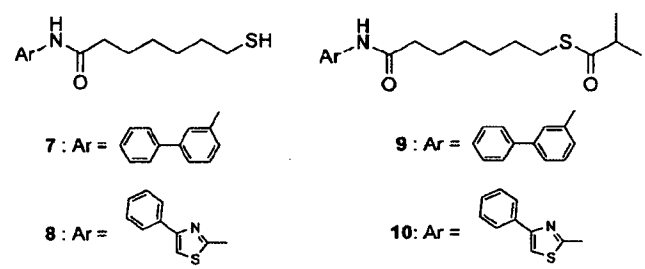

We recently described a series of thiol-based analogues, including **7** (NCH-26) and **8** (NCH-31) (Chart 2), which act as novel non-hydroxamate HDAC inhibitors.[13] Thiols are thought to inhibit HDACs by coordinating the zinc ion which is required for deacetylation of the acetylated lysine substrate. Further, the *S*-isobutyryl prodrugs **9** (NCH-47) and **10** (NCH-51) (Chart 2), which are thought to be hydrolyzed to the free thiols within cells, showed potent cancer cell growth-inhibitory activities.[14] Following these findings, we performed further investigation of thiolate analogues, seeking to find HDAC6-selective inhibitors. We describe here the HDAC6 selectivity of thiolates whose designs were based on the structure of a small-molecular HDAC6-selective substrate.

Results and Discussion

Since HDAC6 has been reported as an α-tubulin deacetylase,[3b,3c] inhibition of HDAC6 and that of other HDACs can be assessed according to the accumulation of acetylated α-tubulin and acetylated histones, respectively, using Western blot analysis. We initially examined the histone/α-tubulin acetylation selectivity of **2**, **9**, and **10** (Figure 1). As reported previously,[11b] **2** caused the accumulation of both acetylated histone H4 and acetylated α-tubulin. Like other non-

* To whom correspondence should be addressed. Tel and fax: +81–52–836–3407; e-mail: suzuki@phar.nagoya-cu.ac.jp; miyata-n@phar.nagoya-cu.ac.jp.

† Graduate School of Pharmaceutical Sciences, Nagoya City University.

‡ RIKEN.

§ CREST Research Project.

[a] Abbreviations: HDAC, histone deacetylase; SIRT, sirtuin; AU, arbitary unit.

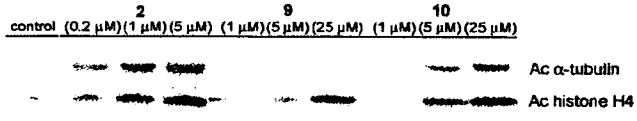

Figure 1. Western blot detection of acetylated α-tubulin and histone H4 levels in HCT116 cells after incubation with compounds **2**, **9**, and **10** for 8 h.

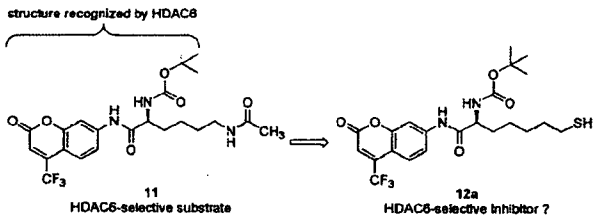

Figure 2. Design of HDAC6-selective inhibitors.

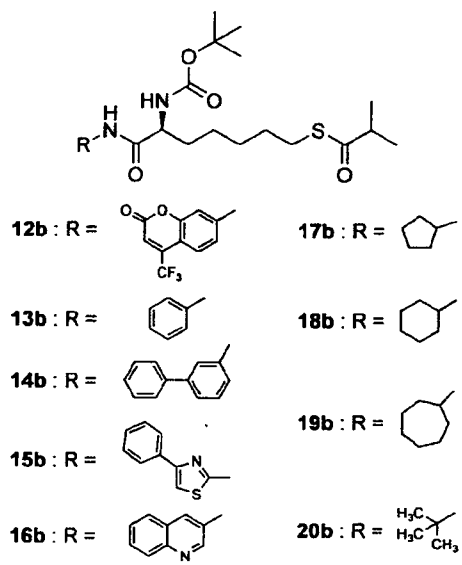

Figure 3. Structures of the thioesters **12b**–**20b**.

hydroxamate HDAC inhibitors, compound **9** selectively caused histone H4 hyperacetylation, which indicates that compound **7** selectively inhibits nuclear HDACs over cytoplasmic HDAC6. However, unlike other non-hydroxamates, compound **10** increased the acetylation state of both histone H4 and α-tubulin. These results suggested that HDAC6-selective inhibitors might be obtained by structural modification of thiolate HDAC inhibitors.

In designing novel HDAC6-selective inhibitors, we focused initially on a small-molecular HDAC6-selective substrate **11**[15] (Figure 2). Jung and co-workers found that compound **11** is selectively deacetylated by HDAC6 in preference to HDAC1 and HDAC3. This indicated that the structure of *N*-Boc and trifluoromethyl coumaryl amide of compound **11** is selectively recognized by HDAC6, and so we considered that compound **12a**, in which the acetamide of **11** is replaced by a thiol, might behave as an HDAC6-selective inhibitor (Figure 2).

Since we used a cellular assay as the first screening, compound **12b** (Figure 3), the *S*-isobutyryl prodrug of compound **12a**, and its derivatives **13b**–**20b** were initially prepared. The route used for synthesis of compounds **12b**–**20b** is shown in Scheme 1. (*S*)-2-Amino-7-bromoheptanoic acid **21**[16] was treated with $(Boc)_2O$ to give *N*-Boc compound **22**. The condensation of carboxylic acid **22** with an appropriate amine afforded amides **23**. Bromides **23** were treated with thioisobutyric acid under alkaline conditions to yield the desired thioesters **12b**–**20b**.

Scheme 1[a]

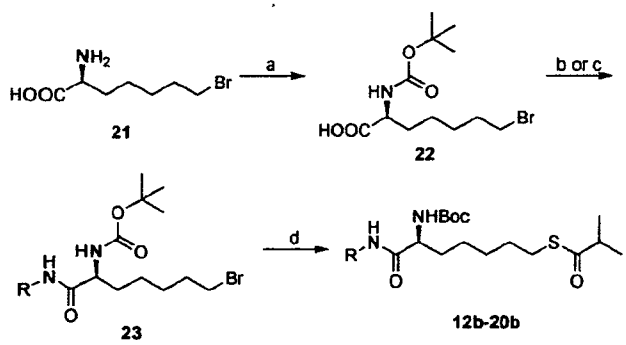

[a] Reagents: (a) $(Boc)_2O$, Et_3N, THF, H_2O, rt, 96%; (b) $ArNH_2$, $POCl_3$, pyridine, −15 °C, 10–48%; (c) RNH_2, 2-(1*H*-benzotriazol-1-yl)-1,1,3,3-tetramethyluroniumhexafluorophosphate, 1-hydroxybenzotriazole hydrate, Et_3N, DMF, rt, 35–63%; (d) thioisobutyric acid, Et_3N, EtOH, rt, 19–58%.

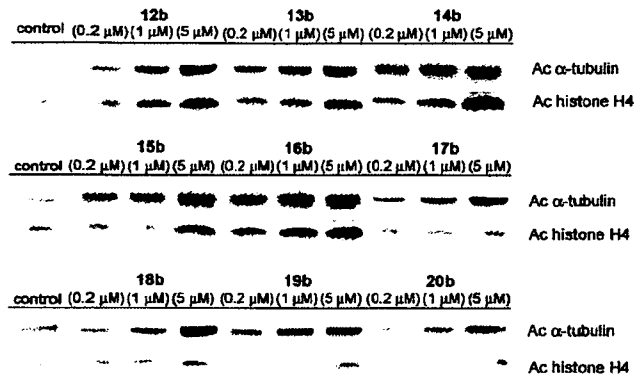

Figure 4. Western blot detection of acetylated α-tubulin and histone H4 levels in HCT116 cells after 8 h treatment with **12b**–**20b**.

We initially evaluated compound **12b** for the accumulation of acetylated α-tubulin and histone H4 using Western blot analysis (Figure 4). Although compound **12b** produced an increase in the accumulation of acetylated α-tubulin as compared with **9** and **10** (Figure 1), the selectivity was insufficient. In an attempt to improve the selectivity of the histone/α-tubulin acetylation, we decided to carry out the structural conversion of compound **12b**. The coumarin structure derived from a substrate for fluorescent enzyme assays was replaced with various aromatic (**13b**–**16b**) or aliphatic (**17b**–**20b**) moieties (Figure 3). Interestingly, although the aromatic compounds **13b**–**16b** did not show high selectivity, the aliphatic compounds **17b**–**20b** produced a dose-dependent increase of α-tubulin acetylation without a major increase in acetylated histone H4 (Figure 4). These results indicated that the aliphatic compounds **17b**–**20b** selectively inhibit HDAC6 in preference to other HDACs in cells. To quantify the selectivity of cyclopentyl **17b**, one of the most active α-tubulin acetylating agents in this series, acetylated α-tubulin and histone H4, were measured over a range of concentrations (Figure 5). The estimated EC_{50} values of cyclopentyl **17b** for α-tubulin acetylation and histone H4 acetylation were 0.23 μM and >32 μM, respectively, and the selectivity index (histone acetylation EC_{50}/α-tubulin acetylation EC_{50}) was >140 which exceeded those of **2** (SI = 2.0) and **6** (SI = 75)[11b] (Figure 5 and Figure 1S of Supporting Information).

To confirm the HDAC6-selectivity of these aliphatic compounds, we performed in vitro enzyme assays. For the enzyme assays, we synthesized compounds **17a**–**19a**, the corresponding thiols of **17b**–**19b**. Compounds **17a**–**19a** were prepared by the

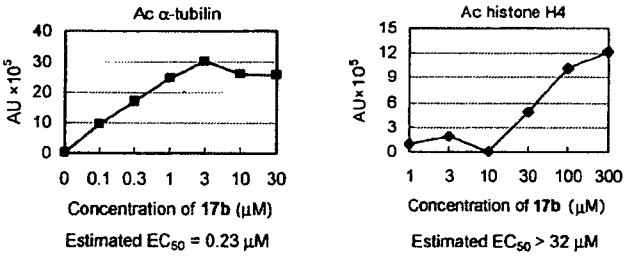

Figure 5. Quantification of acetylated α-tubulin and histone H4 levels in HCT116 cells treated for 8 h with **17b**. Compound **17b** was insoluble in 0.1% DMSO–McCoy5A culture medium at concentrations >300 μM.

Scheme 2[a]

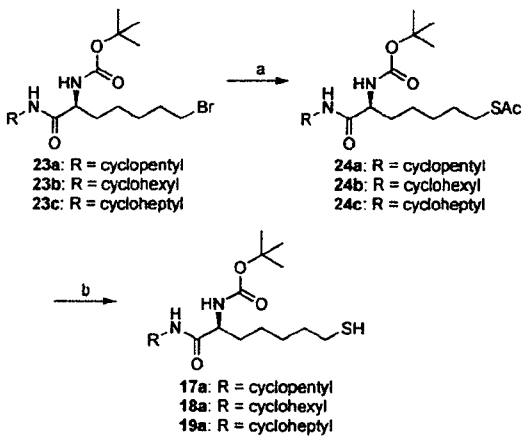

[a] Reagents: (a) KSAc, EtOH, rt, 75–93%; (b) NaOH, H_2O, EtOH, rt, 71–77%.

Table 1. In Vitro HDAC1-, HDAC4-, and HDAC6-Inhibitory Activities of **17a–19a**[a]

	IC_{50} (nM)			selectivity	
compd	HDAC1	HDAC4	HDAC6	HDAC1/ HDAC6	HDAC4/ HDAC6
1	21	34	81	0.26	0.42
6	ND[c]	ND	ND	4[b]	4[b]
7a	1210	1030	29	42	36
8a	1270	1140	36	35	32
9a	900	840	23	39	37

[a] Values are means of at least three experiments. [b] Data taken from the literature (ref 17). [c] ND = No data.

procedure outlined in Scheme 2. Bromides **23** were treated with potassium thioacetate to give compounds **24**, after which hydrolysis of the thioesters under alkaline conditions gave the desired thiols **17a–19a**.

The results of enzyme assays are shown in Table 1. The HDAC6-inhibitory activity of compounds **17a–19a** was greater than that of **1** (IC_{50} of **1** 81 nM, **17a** 29 nM, **18a** 36 nM, **19a** 23 nM). Furthermore, while **1** inhibited HDAC1 and HDAC4 rather than HDAC6 (HDAC1 IC_{50}/HDAC6 IC_{50} = 0.26; HDAC4 IC_{50}/HDAC6 IC_{50} = 0.42), compounds **17a–19a** excellently inhibited HDAC6 in preference to HDAC1 and HDAC4 (HDAC1 IC_{50}/HDAC6 IC_{50} = 35–42; HDAC4 IC_{50}/HDAC6 IC_{50} = 32–37). The HDAC6 selectivity of compounds **17a–19a** is about 10 times higher than that of **6** which showed about only 4-fold selectivity for HDAC6 over HDAC1 and HDAC6 in enzyme assays.[17] These enzyme assays revealed that compounds **17a–19a** are potent and selective inhibitors of HDAC6. The reason that there is essentially no difference in the activity and selectivity of compounds **17a–19a** is unclear, but it is assumable that HDAC6 has a hydrophobic pocket where some sterically bulky alkyl groups can be placed and other HDAC isoforms do not have such a pocket.

In conclusion, we have identified novel HDAC6-selective inhibitors whose designs were based on the structure of the HDAC6-selective substrate **11**. As far as we could determine, they are the first inhibitors that show significant HDAC6-selective inhibition in both cellular and enzyme assays. We have also established that the presence of a bulky alkyl group in these compounds is important for HDAC6-selective inhibition. The structures of the newly discovered HDAC6-selective inhibitors **17–20** are simpler than that of **6** and appear to be suitable as lead structures for the further development of superior HDAC6-selective inhibitors. These findings provide a basis for constructing new tools for probing the biology of HDAC6 and for finding new candidate antitumor agents with potentially fewer side effects.

Acknowledgment. This research was partly supported by Grants-in Aid for Young Scientists (B) from the Ministry of Education, Science, Culture, Sports, Science, Technology, Japan, and grants from the Hori Information Science Promotion Foundation, the Japan Securities Scholarship Foundation, the Tokyo Biochemical Research Foundation, Takeda Science Foundation, the TERUMO Lifescience Foundation and the Program for the Promotion of Fundamental studies in Health Science of the National Institute of Biomedical Innovation (NIBIO), Japan. We thank the Screening Committee of New Anticancer Agents, supported by a Grant-in-Aid for Scientific Research on Priority Area "Cancer" from the Ministry of Education, Culture, Sports, Science and Technology of Japan for HDAC1 inhibition assay results.

Supporting Information Available: Experimental procedures including spectral data for compounds **12–20** and biological methods (PDF). This material is available free of charge via the Internet at http://pubs.acs.org.

References

(1) (a) Grozinger, C. M.; Schreiber, S. L. Deacetylase Enzymes: Biological Functions and the Use of Small-Molecule Inhibitors. *Chem. Biol.* **2002**, *9*, 3–16. (b) Kouzarides, T. Acetylation: a regulatory modification to rival phosphorylation? *EMBO J.* **2000**, *19*, 1176–1179. (c) Kouzarides, T. Histone acetylases and deacetylases in cell proliferation. *Curr Opin. Genet. Dev.* **1999**, *9*, 40–48. (d) Hassig, C. A.; Schreiber, S. L. Nuclear histone acetylases and deacetylases and transcriptional regulation: HATs off to HDACs. *Curr. Opin. Chem. Biol.* **1997**, *1*, 300–308.

(2) (a) Biel, M.; Wascholowski, V.; Giannis, A. Epigenetics-an epicenter of gene regulation: histones and histone-modifying enzymes. *Angew. Chem., Int. Ed. Engl* **2005**, *44*, 3186–3216. (b) Mai, A.; Massa, S.; Rotili, D.; Cerbara, I.; Valente, S.; Pezzi, R.; Simeoni, S.; Ragno, R. Histone deacetylation in epigenetics: an attractive target for anticancer therapy. *Med. Res. Rev.* **2005**, *25*, 261–309. (c) Suzuki, T.; Miyata, N. Epigenetic control using natural products and synthetic molecules. *Curr. Med. Chem.* **2006**, *13*, 935–958. (d) Schaefer, S.; Jung, M. Chromatin modifications as targets for new anticancer drugs. *Arch. Pharm.* **2005**, *338*, 347–357.

(3) (a) Bali, P.; Pranpat, M.; Bradner, J.; Balasis, M.; Fiskus, W.; Guo, F.; Rocha, K.; Kumaraswamy, S.; Boyapalle, S.; Atadja, P.; Seto, E.; Bhalla, K. Inhibition of histone deacetylase 6 acetylates and disrupts the chaperone function of heat shock protein 90: a novel basis for antileukemia activity of histone deacetylase inhibitors. *J. Biol. Chem.* **2005**, *280*, 26729–26734. (b) Hubbert, C.; Guardiola, A.; Shao, R.; Kawaguchi, Y.; Ito, A.; Nixon, A.; Yoshida, M.; Wang, X.; Yao, T. HDAC6 is a microtubule-associated deacetylase. *Nature* **2002**, *417*, 455–458. (c) Matsuyama, A.; Yoshimatsu, Y.; Shimazu, T.; Sumida, Y.; Osada, H.; Komatsu, Y.; Nishino, N.; Khochbin, S.; Horinouchi, S.; Yoshida, M. In vivo destabilization of dynamic microtubules by HDAC6-mediated deacetylation. *EMBO J.* **2002**, *21*, 6820–6831. (d) Kovacs, J. J.; Murphy, P. J.; Gaillard, S.; Zhao, X.; Wu, J. T.; Nicchitta, C. V.; Yoshida, M.; Toft, D. O.; Pratt, W. B.; Yao, T. P. HDAC6 regulates Hsp90 acetylation and chaperone-dependent activation of glucocorticoid receptor. *Mol. Cell* **2005**, *18*, 601–607.

(4) Hideshima, T.; Bradner, J. E.; Wong, J.; Chauhan, D.; Richardson, P.; Schreiber, S. L.; Anderson, K. C. Small-molecule inhibition of proteasome and aggresome function induces synergistic antitumor activity in multiple myeloma. *Proc. Natl. Acad. Sci. U.S.A.* **2005**, *102*, 8567−8572.
(5) (a) Miller, T. A.; Witter, D. J.; Belvedere, S. Histone Deacetylase Inhibitors.*J. Med. Chem.* **2003**, *46*, 5097−5116. (b) Yoshida, M.; Matsuyama. A.; Komatsu, Y.; Nishino, N. From discovery to the coming generation of histone deacetylase inhibitors. *Curr. Med. Chem.* **2003**, *10*, 2351−2358. (c) Miller, T. A. Patent status of histone deacetylase inhibitors. *Expert Opin. Ther. Pat.* **2004**, *14*, 791−804. (d) Weinmann, H.; Ottow, E. Histone deacetylase inhibitors: a survey of recent patents. *Expert Opin. Ther. Pat.* **2005**, *15*, 1677−1690.
(6) (a) Yoshida, M.; Kijima, M.; Akita, T.; Beppu, T. Potent and specific inhibition of mammalian histone deacetylase both in vivo and in vitro by trichostatin A. *J. Biol. Chem.* **1990**, *265*, 17174−17179. (b) Yoshida, M.; Horinouchi, S.; Beppu, T. Trichostatin A and trapoxin: Novel chemical probes for the role of histone acetylation in chromatin structure and function. *BioEssays* **1995**, *17*, 423−430.
(7) (a) Richon, V. M.; Emiliani, S.; Verdin, E.; Webb, Y.; Breslow, R.; Rifkind, R. A.; Marks, P. A. A class of hybrid polar inducers of transformed cell differentiation inhibits histone deacetylases. *Proc. Natl. Acad. Sci. U.S.A.* **1998**, *95*, 3003−3007. (b) Richon, V. M.; Webb, Y.; Merger, R.; Sheppard, T.; Jursic, B.; Ngo, L.; Civoli, F.; Breslow, R.; Rifkind, R. A.; Marks, P. A. Second generation hybrid polar compounds are potent inducers of transformed cell differentiation. *Proc. Natl. Acad. Sci. U.S.A.* **1996**, *93*, 5705−5708.
(8) Komatsu, Y.; Tomizaki, K. Y.; Tsukamoto, M.; Kato, T.; Nishino, N.; Sato, S.; Yamori, T.; Tsuruo, T.; Furumai, R.; Yoshida, M.; Horinouchi, S.; Hayashi, H. Cyclic hydroxamic-acid-containing peptide 31, a potent synthetic histone deacetylase inhibitor with antitumor activity. *Cancer Res.* **2001**, *61*, 4459−4466.
(9) Kijima, M.; Yoshida, M.; Sugita, K.; Horinouchi, S.; Beppu, T.Trapoxin, an antitumor cyclic tetrapeptide, is an irreversible inhibitor of mammalian histone deacetylase. *J. Biol. Chem.* **1993**, *268*, 22429−22435.
(10) Suzuki, T.; Ando, T.; Tsuchiya, K.; Fukazawa, N.; Saito, A.; Mariko, Y.; Yamashita, T.; Nakanishi, O. Synthesis and Histone Deacetylase Inhibitory Activity of New Benzamide Derivatives. *J. Med. Chem.* **1999**, *42*, 3001−3003.
(11) (a) Suzuki, T.; Miyata, N. Non-hydroxamate histone deacetylase inhibitors. *Curr. Med. Chem.* **2005**, *12*, 2867−2880. (b) Wong, J. C.; Hong, R.; Schreiber, S. L. Structural Biasing Elements for In−Cell Histone Deacetylase Paralog Selectivity. *J. Am. Chem. Soc.* **2003**, *125*, 5586−5587. (c) Furumai, R.; Komatsu, Y.; Nishino, N.; Khochbin, S.; Yoshida, M.; Horinouchi, S. Potent histone deacetylase inhibitors built from trichostatin A and cyclic tetrapeptide antibiotics including trapoxin. *Proc. Natl. Acad. Sci. U.S.A.* **2001**, *98*, 87−92. (d) Glaser, K. B.; Li, J.; Pease, L. J.; Staver, M. J.; Marcotte, P. A.; Guo, J.; Frey, R. R.; Garland, R. B.; Heyman, H. R.; Wada, C. K.; Vasudevan, A.; Michaelides, M. R.; Davidsen, S. K.; Curtin, M. L. Differential protein acetylation induced by novel histone deacetylase inhibitors. *Biochem. Biophys. Res. Commun.* **2004**, *325*, 683−690. (e) Suzuki, T.; Matsuura, A.; Kouketsu, A.; Hisakawa, S.; Nakagawa, H.; Miyata, N. Design and synthesis of non-hydroxamate histone deacetylase inhibitors: identification of a selective histone acetylating agent. *Bioorg. Med. Chem.* **2005**, *13*, 4332−4342.
(12) (a) Haggarty, S. J.; Koeller, K. M.; Wong, J. C.; Butcher, R. A.; Schreiber, S. L. Multidimensional Chemical Genetic Analysis of Diversity-Oriented Synthesis-Derived Deacetylase Inhibitors Using Cell-Based Assays. *Chem. Biol.* **2003**, *10*, 383−396. (b) Haggarty, S. J.; Koeller, K. M.; Wong, J. C.; Grozinger, C. M.; Schreiber, S. L. Domain-selective small-molecule inhibitor of histone deacetylase 6 (HDAC6)-mediated tubulin deacetylation. *Proc. Natl. Acad. Sci. U.S.A.* **2003**, *100*, 4389−4394. (c) Stemson, S. M.; Wong, J. C.; Grozinger, C. M.; Schreiber, S. L. Synthesis of 7200 Small Molecules Based on a Substructural Analysis of the Histone Deacetylase Inhibitors Trichostatin and Trapoxin. *Org. Lett.* **2001**, *3*, 4239−4242.
(13) Suzuki, T.; Kouketsu, A.; Matsuura, A.; Kohara, A.; Ninomiya, S.; Kohda, K.; Miyata, N. Thiol-based SAHA analogues as potent histone deacetylase inhibitors. *Bioorg. Med. Chem. Lett.* **2004**, *14*, 3313−3317.
(14) Suzuki, T.; Nagano, Y.; Kouketsu, A.; Matsuura, A.; Maruyama, S.; Kurotaki, M.; Nakagawa, H.; Miyata, N. Novel inhibitors of human histone deacetylases: design, synthesis, enzyme inhibition, and cancer cell growth inhibition of SAHA-based non-hydroxamates. *J. Med. Chem.* **2005**, *48*, 1019−1032.
(15) Heltweg, B.; Dequiedt, F.; Marshall, B. L.; Brauch, C.; Yoshida, M.; Nishino. N.; Verdin, E.; Jung, M. Subtype Selective Substrates for Histone Deacetylases. *J. Med. Chem.* **2004**, *47*, 5235−5243.
(16) Watanabe, L. A.; Jose, B.; Kato, T.; Nishino, N.; Yoshida, M. Synthesis of l-α-amino-ω-bromoalkanoic acid for side chain modification. *Tetrahedron Lett.* **2004**, *45*, 491−494.
(17) Mai, A.; Massa, S.; Pezzi, R.; Simeoni, S.; Rotili, D.; Nebbioso, A.; Scognamiglio, A.; Altucci, L.; Loidl, P.; Brosch, G. Class II (IIa)-Selective Histone Deacetylase Inhibitors. 1. Synthesis and Biological Evaluation of Novel (Aryloxopropenyl)pyrrolyl Hydroxyamides. *J. Med. Chem.* **2005**, *48*, 3344−3353.

JM060554Y

CHEMGX 1 (10) 1033 – 1152 (2006) · ISSN 1860-7179 · Vol. 1 · No. 10 · October, 2006

CHEMMEDCHEM

CHEMISTRY ENABLING DRUG DISCOVERY

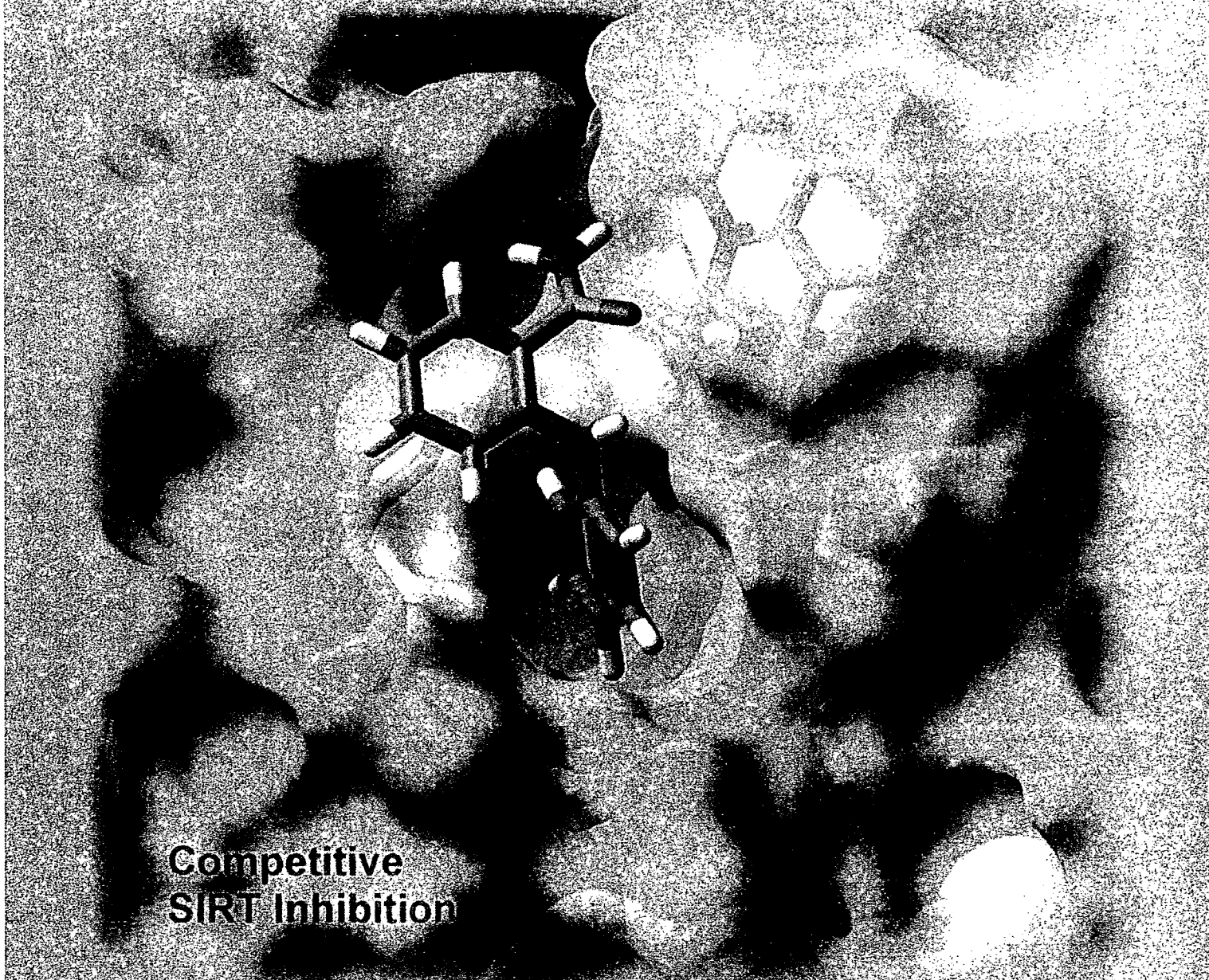

10/2006

Minireview: lipoxidation-derived reactive carbonyl species as potential drug targets

Original Contributions: predicting compound selectivity by self-organizing maps, 2-anilinobenzamides as SIRT inhibitors, MT_1-agonist/MT_2-antagonist melatonin receptor ligands, ferrocenyl-chalcone and ferrocenyl-pyrazoline glycoside derivatives, and more

Now in MEDLINE!

EUChemSoc

WILEY-VCH

CHEMMEDCHEM

CHEMISTRY ENABLING DRUG DISCOVERY

Table of Contents

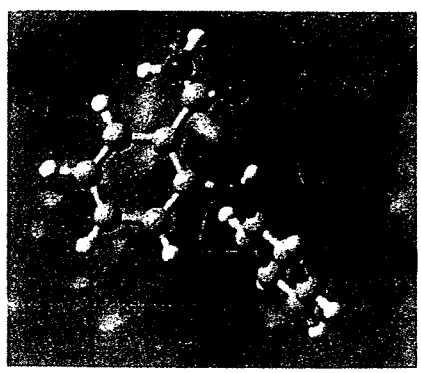

SIRTs, class III histone deacetylases, have been suggested to be associated with certain diseases such as cancer and HIV. Thus, SIRT inhibitors are of interest not only to elucidate the biological functions of the enzyme, but also as potential therapeutic agents. 2-Anilinobenzamide was identified in a nocotinamide- and benzamide-focused compound library as a novel SIRT inhibitor. This compound caused the accumulation of acetylated p53 in HCT116 cells.

WILEY-VCH

DOI: 10.1002/cmdc.200600162

2-Anilinobenzamides as SIRT Inhibitors

Takayoshi Suzuki,* Keiko Imai, Hidehiko Nakagawa, and Naoki Miyata*[a]

Yeast silent information regulator 2 (Sir2) proteins are responsible for the establishment, maintenance, and regulation of gene silencing at mating type loci, telomeres, and rDNA and they act in this capacity by changing chromatin into a transcriptionally inactive state.[1–5] Transcriptional silencing by Sir2 is linked to its deacetylation of the acetylated lysine residues in the N-terminal tails of the histones in chromatin.[6,7] Thus, human SIRT1–7, homologues of the yeast Sir2 proteins, are categorized as Class III histone deacetylases (HDACs).[8] However, the target of SIRT regulatory deacetylation is not limited to histones. For example, SIRT1 catalyzes the deacetylation of p53,[9–11] and SIRT2 deacetylates α-tubulin.[12] Although the functions of SIRTs have not yet been determined, they have been suggested to be associated with certain disease states such as cancer[13,14] and HIV infection.[15] Therefore, SIRT inhibitors are of interest not only as tools for elucidating in detail the biological functions of the enzyme, but can also be considered as potential therapeutic agents.[16]

In contrast to Class I and Class II HDACs, which are zinc-dependent deacetylases, deacetylation by Class III HDACs is dependent on NAD^+.[17,18] In the deacetylation reaction of SIRTs, NAD^+ is hydrolyzed to release nicotinamide and the acetyl group of the acetylated lysine substrate is transferred to cleaved NAD^+, generating *O*-acetyl-ADP ribose.[19,20] To date, several classes of Sir2 or SIRT inhibitors have been reported (Figure 1).[14,15,18,21–26] Among these, nicotinamide is a potent SIRT inhibitor and it has been proposed that it inhibits SIRTs by binding to a conserved pocket adjacent to the NAD^+ binding pocket, thereby blocking NAD^+ hydrolysis.[18,21] EX-527, a recently reported SIRT1-selective inhibitor, is thought to inhibit SIRT1 by occupying the nicotinamide binding pocket.[22] Another SIRT inhibitor, carba-NAD^+, which is a nonhydrolyzable NAD^+ analogue, has been reported to inhibit a Sir2 homologue (HST2) by competing with NAD^+.[18] Very recently, cambinol has been reported as a SIRT1 and SIRT2 inhibitor that is competitive with histone H4-peptide substrates.[14]

Previous reports regarding SIRT inhibitors[18,21,22] suggested the presence of small-molecule inhibitors in a chemical library enriched with the structural families of nicotinamide and benzamide, which were expected to inhibit SIRTs by occupying NAD^+- or nicotinamide-binding pockets. We therefore evaluated the SIRT1 inhibition activity of our in-house compound library comprised of nicotinamide and benzamide derivatives (Figure 2) at a concentration of 300 μM, and the strongest inhibition was observed with 2-anilinobenzamide **7** (Table 1).

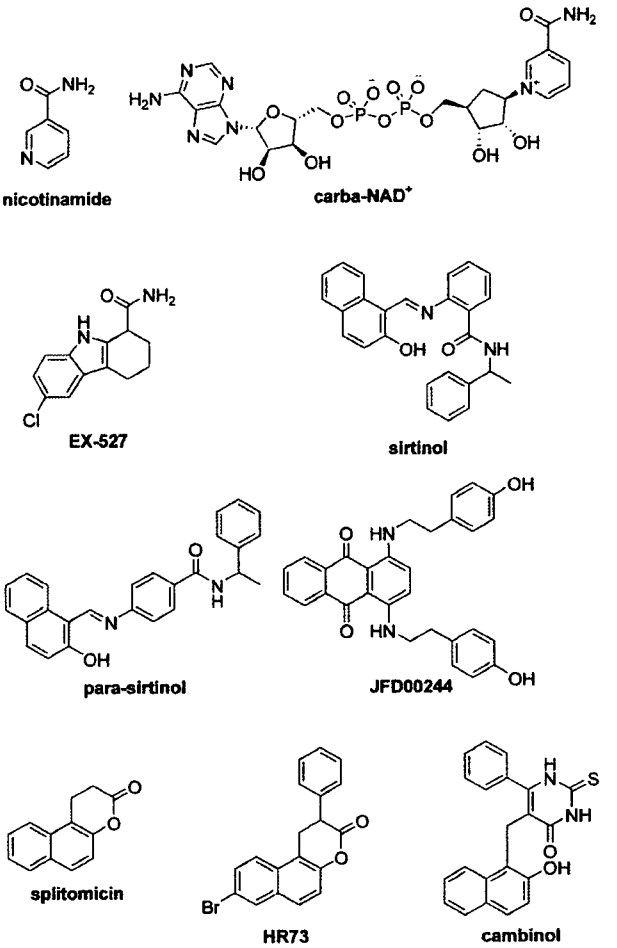

Figure 1. Sir2 and SIRT inhibitors.

To study the preliminary structure–activity relationship (SAR) of 2-anilinobenzamide derivatives, we prepared compounds **19–21** according to the route shown in Scheme 1. Carboxylic acid **22** was converted to *N,O*-dimethyl compound **23** by reac-

Table 1. SIRT1 inhibition data for compounds **1–18**[a]

Compd	Inhibition at 300 μM [%]	Compd	Inhibition at 300 μM [%]
1	0±7.2	**10**	45±1.1
2	72±4.3	**11**	38±2.4
3	4.6±5.5	**12**	0±1.6
4	42±6.5	**13**	37±9.6
5	52±28	**14**	37±2.8
6	42±14	**15**	32±5.4
7	100±2.8	**16**	47±6.1
8	8.4±8.3	**17**	13±9.3
9	47±16	**18**	3.1±9.7

[a] Values are means ±SD determined from at least three experiments.

[a] *Dr. T. Suzuki, K. Imai, Dr. H. Nakagawa, Prof. N. Miyata*
Graduate School of Pharmaceutical Sciences
Nagoya City University
3-1 Tanabe-dori, Mizuho-ku, Nagoya, Aichi 467-8603 (Japan)
Fax: (+81) 52-836-3407
E-mail: suzuki@phar.nagoya-cu.ac.jp; miyata-n@phar.nagoya-cu.ac.jp

Supporting information for this article is available on the WWW under http://www.chemmedchem.org or from the author. Supporting information includes experimental procedures and characterization data for compounds **19**, **20**, and **21**.

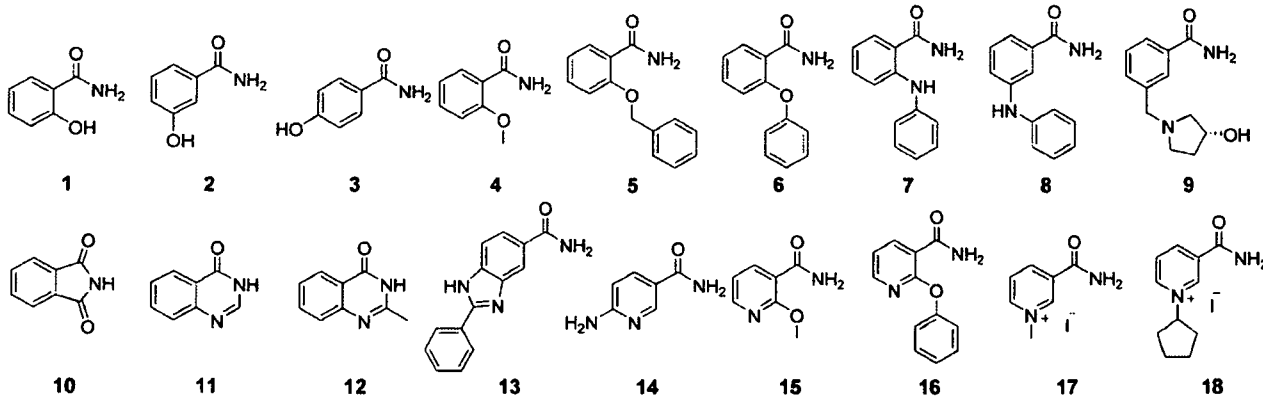

Figure 2. Examples of our benzamide- and nicotinamide-focused library.

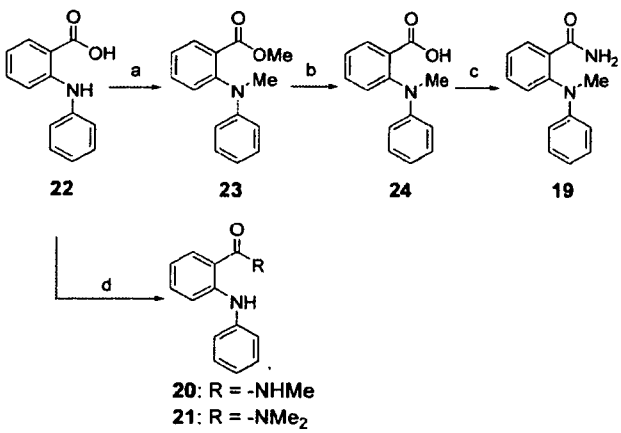

Scheme 1. Reagents and conditions: a) 1) NaH, DMF, RT; 2) MeI, DMF, 80 °C, 99%; b) NaOH, MeOH, H_2O, RT, 99%; c) NH_4Cl, Et_3N, EDCI, HOBt, THF, RT, 69%; d) $MeNH_2$·HCl or Me_2NH·HCl, Et_3N, EDCI, HOBt, THF, RT, 60% for **20**, 37% for **21**.

tion with methyl iodide in the presence of sodium hydride. Hydrolysis of the methyl ester of **23** gave *N*-methyl 2-anilinobenzoic acid **24**. Coupling between carboxylic acids **22**, **24**, and an appropriate amine afforded the desired benzamides **19–21**.

The results of the SIRT1 inhibition assay for compounds **6–8** and **19–22** are summarized in Table 2. Compound **7** exhibited an IC_{50} of 17 μM (see Figure S1 of Supporting Information) and its activity is comparable to that of nicotinamide. We initially tested the activity of compound **8**, the meta isomer of compound **7**, but it was found to be a much weaker inhibitor. We then examined the activity of compounds **6** and **19**, in which the NH group of compound **7** is replaced with an ether and NMe group, respectively. While ether **6** was totally inactive, *N*-methyl compound **19** slightly reduced potency. As for the conversion of the amide moiety, *N*-methyl amide **20** and *N,N*-dimethyl amide **21** significantly reduced the activity, whereas the potency of carboxylic acid **22** was maintained to some extent. The fact that carboxylic acid **22** displayed SIRT1 inhibitory activity was very surprising because the corresponding carboxylic acid derivatives of nicotinamide and EX-527 did not show any activity.[21,22] This indicated that compound **7** might inhibit SIRT1 in a manner different from nicotinamide and EX-527, although the structure of **7** and EX-527 is similar.

The unexpected SAR in the SIRT1 inhibition assay prompted us to investigate the SIRT1 inhibitory mechanism of compound **7**. We performed an enzyme kinetic assay (Lineweaver–Burk plot) using various concentrations of inhibitor **7** (Figure 3). Interestingly, the data from this study established that compound **7** engages in noncompetitive inhibition with NAD^+ and competitive inhibition with the acetylated lysine substrate.

Since compound **7** proved to be competitive with the acetylated lysine substrate and to act within the active site of SIRT1, the lowest energy conformation of **7** was obtained when it was docked into a model based on the crystal structure of yeast HST2 (PDB code 1Q1A),[20] a homologue of Sir2, as calculated using the software packages Glide 3.5 and MacroModel 8.1 (Figure 4). An inspection of the HST2/**7** complex suggests

Table 2. SIRT1 inhibition data for compounds **6–8** and **19–22**[a]

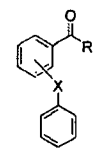

Compound	R	X	Position of XPh	Inhibition at 100 μM [%]	IC_{50} [μM]
nicotinamide				72 ± 11	25 ± 5.1
7	$-NH_2$	-NH-	*ortho*	81 ± 13	17 ± 1.8
6	$-NH_2$	-O-	*ortho*	4.3 ± 0.81	> 100
8	$-NH_2$	-NH-	*meta*	4.1 ± 1.4	> 100
19	$-NH_2$	-NMe-	*ortho*	62 ± 6.4	75 ± 5.6
20	-NHMe	-NH-	*ortho*	19 ± 1.2	> 100
21	$-NMe_2$	-NH-	*ortho*	39 ± 3.9	> 100
22	-OH	-NH-	*ortho*	52 ± 5.2	68 ± 2.9

[a] Values are means ± SD determined from at least three experiments.

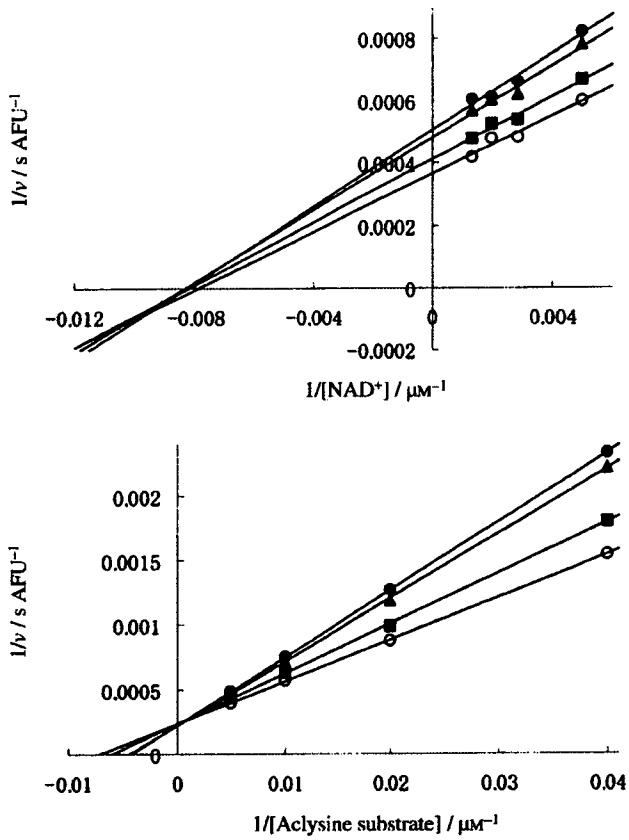

Figure 3. Reciprocal rate against reciprocal NAD^+ concentration (top) and acetylated lysine substrate (bottom) in the presence of 300 (●), 150 (▲), 50 (■), and 0 (○) μM of **7**.

that the NH_2 group and the CO group of **7** form hydrogen bonds with the backbone carbonyl of Ala 227 and with the backbone amine of Tyr 229, and the phenyl group of **7** blocks the entrance of the histone H4-binding pocket by interacting with hydrophobic amino acid residues (Val 182, Phe 184, Gly 185, Leu 188, Val 228, and Pro 238). In addition, an intramolecular hydrogen bond was observed between the CO and NH group of **7**. The results of the in vitro SAR and computational studies imply the importance of the conformation of the inhibitors. Specifically, conformation A of **7** is more stable than conformation B of **7** because of the intramolecular hydrogen bond between its CO and NH group (Figure 5). As the amide group of conformation A of **7** can form hydrogen bonds with the backbone amides of SIRT1, it would appear that compound **7** can strongly inhibit SIRT1. In contrast, conformation B of ether **6** is more stable than conformation A of **6** because of the intramolecular hydrogen bond between its NH group and oxygen atom. The amide group of conformation B of **6** cannot interact with the backbone amides of SIRT1, and this might be the reason that compound **6** lost SIRT1 inhibitory activity. In the case of *N*-methyl compound **19**, conformation A of **19** is more stable than conformation B of **19** due to steric repulsion of the NH group, pushing it away from the *N*-methyl group. Therefore, as with compound **7**, compound **19** can form hydrogen bonds with backbone amides of SIRT1 and this might be the reason that compound **19** showed a certain level of SIRT1-inhibitory activity.

To examine the isoform selectivity of compound **7**, we conducted enzyme assays using SIRT1, SIRT2, and SIRT3. Compound **7** showed about 4-fold and 14-fold selectivity for SIRT1 over SIRT 2 and SIRT3, respectively (IC_{50} for SIRT2 = 74 μM; IC_{50} for SIRT3 = 235 μM). In addition, compound **7** did not inhibit class I and class II HDACs at a concentration of 1000 μM.

To explore the potential for compound **7** to block SIRT1 activity in cells, we performed a cellular assay using western blot analysis. Since SIRT1 is known to catalyze the deacetylation of p53 on DNA damage,[9-11] the acetylation level of p53 in HCT116 cells after etoposide-induced DNA damage was analyzed.[27] As can be seen from Figure 6, elevated and dose-dependent levels of acetylated p53 were observed. These results suggested that compound **7** inhibits SIRT1 in cells.

In summary, to discover novel SIRT inhibitors, we evaluated a nicotinamide- and benzamide-focused chemical library to detect SIRT1 inhibition, and found 2-anilinobenzamide **7** to be a novel SIRT inhibitor. Although the structure of **7** is similar to that of EX-527, that of the SAR is not. The results of kinetic enzyme assays made it clear that compound **7** competes with the acetylated lysine substrate, whereas it has been reported that EX-527 does not.[21] Molecu-

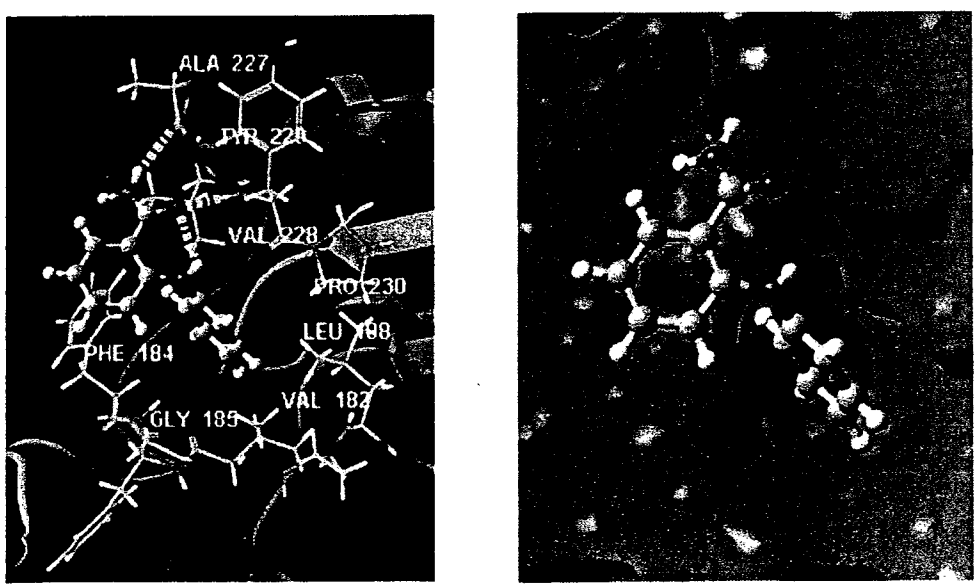

Figure 4. View of the conformation of **7** (ball and stick) docked into the yeast Hst2 (homologue of SIRTs) catalytic core. Residues 5 Å from **7** are displayed in the wire graphic (left) and the surface of the enzyme is displayed in the background (right).

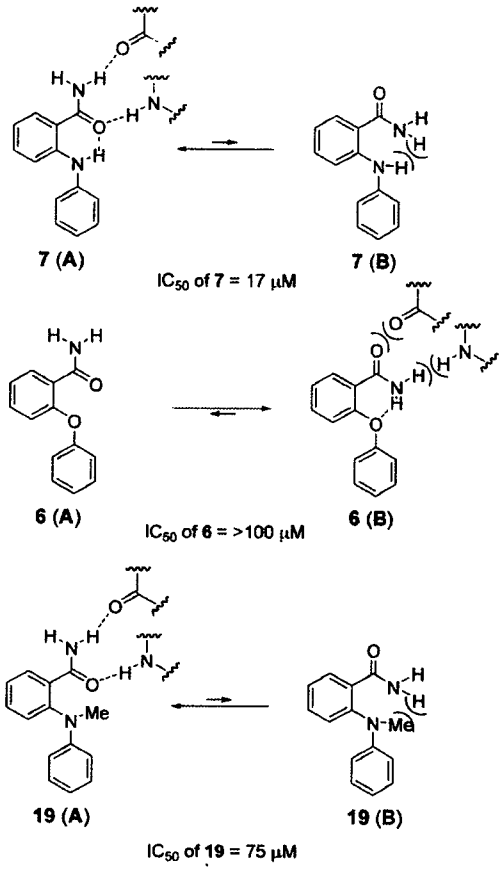

Figure 5. The relationship between SIRT1 inhibitory activity and the stable conformation of compounds **7**, **6**, and **19**.

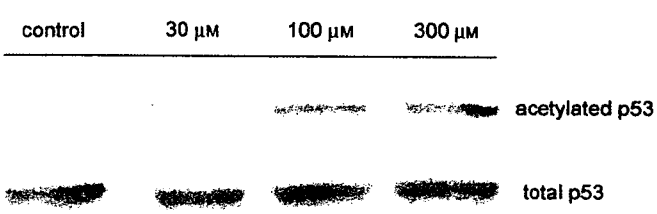

Figure 6. Western blot detection of acetylated p53 levels in HCT116 cells after an 8 h incubation with 20 μM of etoposide and various concentrations of compound **7**.

lar modeling suggests the significance of the conformation of inhibitors and the formation of hydrogen bonds between inhibitors and SIRTs. Compound **7** also caused p53 acetylation in cells, which would be the result of SIRT1 inhibition. These findings provide a basis for developing new tools for probing the biology of SIRTs and for finding new candidate therapeutic agents. Further investigations pertaining to **7** are progressing and will be reported in due course.

Acknowledgements

This research was partly supported by Grants-in Aid for Young Scientists (B) from the Ministry of Education, Science, Culture, Sports, Science, Technology, Japan, and grants from the Hori Information Science Promotion Foundation, the Japan Securities Scholarship Foundation, the Tokyo Biochemical Research Foundation, Takeda Science Foundation and the TERUMO Life Science Foundation.

Keywords: focused chemical library · kinetic analysis · p53 acetylation · SIRT inhibitors · structure–activity relationships

[1] D. E. Gottschling, *Curr. Biol.* **2000**, *10*, R708.
[2] D. Shore, *Proc. Natl. Acad. Sci. USA* **2000**, *97*, 14030.
[3] K. G. Tanner, J. Landry, R. Sternglanz, J. M. Denu, *Proc. Natl. Acad. Sci. USA* **2000**, *97*, 14178.
[4] S. M. Gasser, M. M. Cockell, *Gene* **2001**, *279*, 1.
[5] M. Biel, V. Wascholowski, A. Giannis, *Angew. Chem.* **2005**, *117*, 3248; *Angew. Chem. Int. Ed.* **2005**, *44*, 3186.
[6] L. N. Rusche, A. L. Kirchmaier, J. Rine, *Annu. Rev. Biochem.* **2003**, *72*, 481.
[7] R. M. Anderson, K. J. Bitterman, J. G. Wood, O. Medvedik, D. A. Sinclair, *Nature* **2003**, *423*, 181.
[8] S. Khochbin, A. Verdel, C. Lemercier, D. Seigneurin-Berny, *Curr. Opin. Genet. Dev.* **2001**, *11*, 162.
[9] J. Luo, A. Y. Nikolaev, S. Imai, D. Chen, F. Su, A. Shiloh, L. Guarente, W. Gu, *Cell* **2001**, *107*, 137.
[10] H. Vaziri, S. K. Dessain, E. Ng Eaton, S. I. Imai, R. A. Frye, T. K. Pandita, L. Guarente, R. A. Weinberg, *Cell* **2001**, *107*, 149.
[11] E. Langley, M. Pearson, M. Faretta, U. M. Bauer, R. A. Frye, S. Minucci, P. G. Pelicci, T. Kouzarides, *EMBO J.* **2002**, *21*, 2383.
[12] B. J. North, B. L. Marshall, M. T. Borra, J. M. Denu, E. Verdin, *Mol. Cell* **2003**, *11*, 437.
[13] J. Ford, M. Jiang, J. Milner, *Cancer Res.* **2005**, *65*, 10457.
[14] B. Heltweg, T. Gatbonton, A. D. Schuler, J. Posakony, H. Li, S. Goehle, R. Kollipara, R. A. Depinho, Y. Gu, J. A. Simon, A. Bedalov, *Cancer Res.* **2006**, *66*, 4368.
[15] S. Pagans, A. Pedal, B. J. North, K. Kaehlcke, B. L. Marshall, A. Dorr, C. Hetzer-Egger, P. Henklein, R. Frye, M. W. McBurney, H. Hruby, M. Jung, E. Verdin, M. Ott, *PLoS Biol.* **2005**, *3*, e41.
[16] T. Suzuki, N. Miyata, *Curr. Med. Chem.* **2006**, *13*, 935.
[17] S. Imai, C. M. Armstrong, M. Kaeberlein, L. Guarente, *Nature* **2000**, *403*, 795.
[18] J. Landry, J. T. Slama, R. Sternglanz, *Biochem. Biophys. Res. Commun.* **2000**, *278*, 685.
[19] A. A. Sauve, V. L. Schramm, *Biochemistry* **2003**, *42*, 9249.
[20] K. Zhao, R. Harshaw, X. Chai, R. Marmorstein, *Proc. Natl. Acad. Sci. USA* **2004**, *101*, 8563.
[21] K. J. Bitterman, R. M. Anderson, H. Y. Cohen, M. Latorre-Esteves, D. A. Sinclair, *J. Biol. Chem.* **2002**, *277*, 45099.
[22] A. D. Napper, J. Hixon, T. McDonagh, K. Keavey, J. F. Pons, J. Barker, W. T. Yau, P. Amouzegh, A. Flegg, E. Hamelin, R. J. Thomas, M. Kates, S. Jones, M. A. Navia, J. O. Saunders, P. S. DiStefano, R. Curtis, *J. Med. Chem.* **2005**, *48*, 8045.
[23] C. M. Grozinger, E. D. Chao, H. E. Blackwell, D. Moazed, S. L. Schreiber, *J. Biol. Chem.* **2001**, *276*, 38837.
[24] A. Mai, S. Massa, S. Lavu, R. Pezzi, S. Simeoni, R. Ragno, F. R. Mariotti, F. Chiani, G. Camilloni, D. A. Sinclair, *J. Med. Chem.* **2005**, *48*, 7789.
[25] A. J. Tervo, S. Kyrylenko, P. Niskanen, A. Salminen, J. Leppanen, T. H. Nyronen, T. Jarvinen, A. Poso, *J. Med. Chem.* **2004**, *47*, 6292.
[26] A. Bedalov, T. Gatbonton, W. P. Irvine, D. E. Gottschling, J. A. Simon, *Proc. Natl. Acad. Sci. USA* **2001**, *98*, 15113.
[27] Etoposide was used to cause DNA damage and subsequent induction of p53. In the absence of etoposide, the induction of p53 was not observed (data not shown).

Received: June 29, 2006
Published online on September 20, 2006

Available online at www.sciencedirect.com
ScienceDirect
Bioorganic & Medicinal Chemistry Letters
ELSEVIER
Bioorganic & Medicinal Chemistry Letters 16 (2006) 5939–5942

Hydroxyl radical scavenging by edaravone derivatives: Efficient scavenging by 3-methyl-1-(pyridin-2-yl)-5-pyrazolone with an intramolecular base

Hidehiko Nakagawa,* Ryo Ohyama, Ayako Kimata, Takayoshi Suzuki and Naoki Miyata*

Graduate School of Pharmaceutical Sciences, Nagoya City University, 3-1, Tanabe-dori, Mizuho-ku, Nagoya, Aichi 467-8603, Japan

Received 1 August 2006; revised 31 August 2006; accepted 2 September 2006
Available online 25 September 2006

Abstract—We synthesized various 3-methyl-1-phenyl-5-pyrazolone (edaravone) derivatives and evaluated their oxidation potential and hydroxyl radical scavenging activity. It was found 3-methyl-1-(pyridin-2-yl)-5-pyrazolone had a much higher ability to scavenge the radical than did edaravone itself. Its efficient radical scavenging activity was assumed to be due to the increase of its anion form, an active form, by a hydrogen-bonded intramolecular base.

Reactive oxygen species are involved in many pathological conditions such as ischemic-reperfusion injury,[1,2] cellular aging,[3] and progression of arteriosclerosis.[4]

Recently, a new pyrazolin compound, edaravone (3-methyl-1-phenyl-2-pyrazolin-5-one, also known as MCI-186, Fig. 1) has been developed as a medical drug for brain ischemia,[5,6] and has been reported to be effective for myocardial ischemia as well.[7] Edaravone (**A**) is known to be an efficient antioxidant, which is considered to be the basis of its protective effect against ischemia. Its enolate form (**B**) can interact with both peroxyl ($LOO^{\cdot}$) and hydroxyl radicals ($^{\cdot}OH$), followed by the formation of a stable oxidation product (OPB: 2-oxo-3-(phenylhydrazono)-butanoic acid) through a radical intermediate[8,9] (Fig. 1).

We were encouraged to study the structure–activity relationship (SAR) as a means of characterizing the structural features of edaravone and optimizing the structure with regard to its radical scavenging activity in an aqueous solution. For this purpose, we synthesized edaravone derivatives with various substituents such as electron-withdrawing groups (EWG), electron-donating groups (EDG), and π-conjugated groups at the 1-, 3-, or 4-positions of the pyrazolone ring (see supporting information).[10] Oxidation potentials of the synthesized pyrazolone derivatives were measured by cyclic voltammetry (CV) in an aqueous solution, and their hydroxyl radical scavenging activity was evaluated using the electron spin resonance (ESR) spin-trapping method.

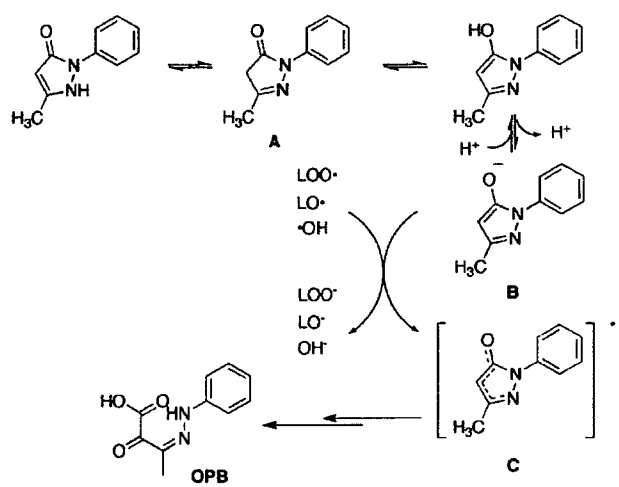

Figure. 1. Reaction mechanisms of edaravone (**A**) with free radicals. OPB; 2-oxo-3-(phenylhydrazono)-1-butanoic acid.

Keywords: Pyrazolone derivatives; Antioxidant; Anion form amount.
* Corresponding authors. Tel./fax: +81 52 836 3407; e-mail addresses: deco@phar.nagoya-cu.ac.jp; miyata-n@phar.nagoya-cu.ac.jp

Table 1. Oxidation potentials (E_{pa}) of the edaravone derivatives

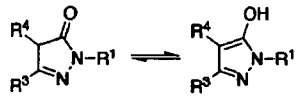

Compound	R^1	R^3	R^4	E_{pa}[a] (mV)	pH
A (edaravone)	Ph–	CH_3–	H	483	7.0
A (edaravone)	Ph–	CH_3–	H	480	7.8
1	4-CH_3OPh–	CH_3–	H	678	7.8
2	4-ClPh–	CH_3–	H	473	7.4
3	Cyclohexyl–	CH_3–	H	549	7.4
4	2-Pyridinyl–	CH_3–	H	483	7.0
5	Ph–	CF_3–	H	673	7.6
6	Ph–	Ph–	H	397	7.6
7	Ph–	4-NO_2Ph–	H	419	7.4
8	Ph–	4-CH_3OPh–	H	397	7.8
9	Ph–	CH_3OCONH–	H	454	7.8
10	Ph–	PhOCONH–	H	397	7.0
11	Ph–	CyclopentylNHCONH–	H	372	7.8
12	Ph–	Isopropenyl–	H	387	7.4
13	Ph–	Bn–	H	269	>8.0
14	Ph–	CH_3–	Isobutyl–	262	>8.0
15	Ph–	CH_3–	Ph–	227	7.6
16	Ph–	CH_3–	Cyclopropyl–	275	7.8
17	Ph–	CH_3–	PhCO–	640	7.0
18	4-NO_2Ph–	CH_3–	H	525	7.6

Conditions for measurement: 10 mM sample in 50 mM NaCl. Working electrode; Pt, reference electrode; Ag^+/AgCl, counter electrode; Pt, scan speed; 50 mV/s, Scan range −0.2 to 1.0 V.

[a] The oxidation potentials were expressed versus Ag^+/AgCl.

One-electron oxidation potentials (E_{pa}) of all the synthesized derivatives were measured in a 50 mM NaCl solution (Table 1). Oxidation currents were observed with all the tested compounds, but were irreversible, probably because the one-electron oxidation products were unstable and converted to degraded compounds as reported.[8,9] Because of the poor solubility of several derivatives in the neutral aqueous solution, the solutions were slightly basified using aqueous NaOH to solubilize these compounds.

Although the derivatives with strong EWGs, such as compound **5** with a trifluoromethyl group and **17** with a benzoyl group, had relatively higher oxidation potentials as expected, the other derivatives showed a wide variety of oxidation potentials regardless of the electronic properties of the substituents (Table 1). It is possible that the oxidation potentials were not only affected by the electron density on the pyrazolone ring but also by the stability of the resulting radical species (**C**) with conjugated π-orbitals on the substituent. In comparison, among the positions of the substituents, the substitution at position 1 did not positively affect the reduction of the oxidation potential, whereas that at the position 4 seemed to be more effective (Fig. 2).

The radical scavenging activity was evaluated by the ESR spin-trapping method with 5,5-dimethyl-1-pyrroline-*N*-oxide (DMPO) as a spin trap. Hydroxyl radicals were generated by UV irradiation (2000 J/cm^2) of the hydrogen peroxide solution containing DMPO and edaravone derivatives.[11,12] The inhibitory effect of the derivatives on the formation of hydroxyl radical adducts of DMPO was used as a measure of the radical scavenging activity. The IC_{50} values were determined for seven of nineteen derivatives with diverse oxidation potentials (**1A**, **5**, **10**, **15**, **16**, **17**, and **18**). The relationship between the IC_{50} value and the oxidation potential was not simply proportional, but showed a V-shaped correlation (Fig. 3). Edaravone (**A**), which had an oxidation potential of 483 mV (vs Ag^+/AgCl), showed the lowest IC_{50} value among the seven derivatives tested.

The edaravone anion (**B**) is reported to be an active form in scavenging free radicals by a one-electron-transferring mechanism.[13,14] Actually, in the case of one-electron oxidation of edaravone with 2,2'-azobis(2,4-dimethylvaleronitrile) (AMVN), a radical initiator, the oxidation rate was increased in a pH-dependent manner in methanol/buffer solutions.[8] Therefore, the amount of the anionic form of the synthesized derivatives is important for scavenging activities. On the other hand, the electron density of the pyrazolone moiety is also important for one-electron oxidation reactivity. The relatively electron-rich substituents on the pyrazolone ring may lower the oxidation potential, but concomitantly decrease the amount of their anionic form by protonation due to the increasing partial negative charges. In contrast, electron-poor substituents may increase the amount of the anionic form but enlarge the oxidation potential. As shown in Table 2 and Figure 3, edaravone had almost the best oxidation potential for hydroxyl radical scavenging under our experimental conditions, an activity in which the oxidation potential and the amount of the anion form may be well balanced.

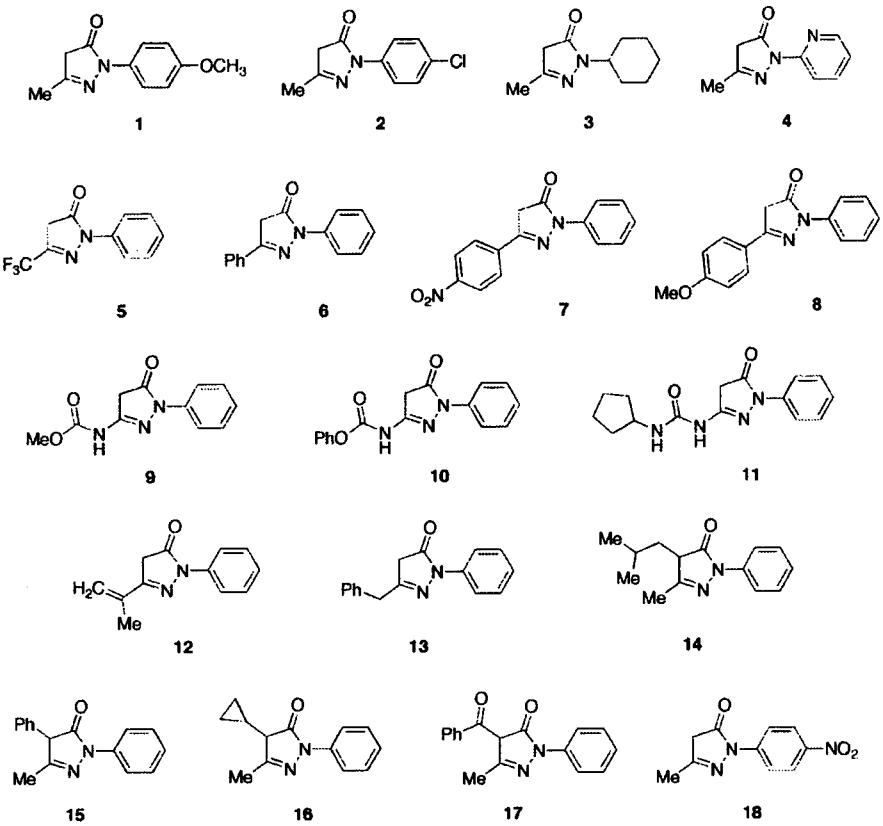

Figure. 2. Structures of edaravone derivatives synthesized in this study.

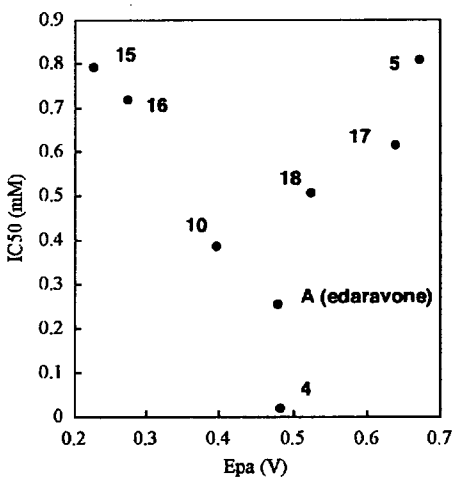

Figure. 3. The relationship between oxidation potentials (E_{pa}) and IC_{50} values. Each data point represents a specific derivative with its number along side.

As reported,[10] edaravone derivatives with lipophilic substituents on the phenyl group at position 1 of the pyrazolone ring showed higher inhibitory activity against the lipid peroxidation, which was likely due to the increasing concentrations of the derivatives in the lipid phase. With aqueous solutions, our results suggested that the increase of the anionic form of the derivatives appeared to be an important requirement for efficient radical scavenging.

Since the pK_a values of the derivatives in the aqueous solutions were hardly evaluated due to the poor solubility of the derivatives in neutral and acidic solutions, we referred to the CAS database and only used the data for the comparison of the relative stability of the deprotonated form. For novel compounds, pK_a values were estimated by calculating free energy changes in their deprotonation with density functional theory (B3LYP/6-31G*) on Spartan 02 or 04 software (Wavefunction, Inc. Irvine, CA, USA) (see supporting information). The calculated pK_a values were found to be roughly higher for derivatives with lower oxidation potentials than that of edaravone, implying that the amount of the anionic form may be related to the radical scavenging activity of derivatives with lower oxidation potentials than that of edaravone.

In the light of the properties clarified above, the increase in the anionic form without concomitant positive shift of the oxidation potential may be effective for efficient one-electron radical reduction. Although one-electron oxidation of a derivative apparently occurs in its anion form, deprotonation of a derivative does not affect its potential of one-electron oxidation, but does affect its oxidation current. We next focused on compound **4**, which has a pyridin-2-yl moiety as an intramolecular base at position 1 of the pyrazolone ring. This basic function may facilitate the partial deprotonation from the pyrazolone ring moiety. As expected, its IC_{50} value was 13.9 times smaller than that of edaravone with almost the same oxidation

Table 2. Hydroxyl radical scavenging activity (IC_{50}) of the edaravone derivatives

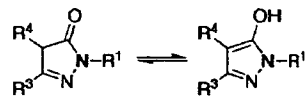

Compound	R^1	R^3	R^4	IC_{50} (mM)
A (edaravone)	Ph–	CH_3–	H	0.25
4	2-Pyridinyl–	CH_3–	H	0.018
5	Ph–	CF_3–	H	0.81
10	Ph–	PhOCONH–	H	0.38
15	Ph–	CH_3–	Ph–	0.79
16	Ph–	CH_3–	Cyclopropyl–	0.72
17	Ph–	CH_3–	PhCO–	0.61
18	4-NO_2Ph–	CH_3–	H	0.50

Conditions for measurement: a mixture of 25 mM H_2O_2, 25 mM DMPO, and a compound was irradiated with UV. ESR spectrometer parameters were: microwave power, 10 mW; modulation width, 0.063 mT; time constant, 0.03 s; sweep width, 7.5 mT; sweep time, 1 min; gain, 320.

potential (Table 2 and Fig. 3). This implies that the pyridin-2-yl function partially deprotonated from the pyrazolone ring by forming an intramolecular hydrogen-bond without a marked decrease in the electron density of the pyrazolone ring. Supporting this idea, it was confirmed by ^1H NMR analysis that **4** was in its enol form in $CDCl_3$ solution, in which a singlet methyne proton (δ 5.4) and a broadened enol proton (δ 12.7) were observed instead of two methylene protons (δ 3–4) of the pyrazolone ring (see supporting information).

In conclusion, we determined the oxidation potential and hydroxyl radical scavenging activity of various edaravone-related derivatives in an aqueous solution, and analyzed their characteristics as free radical scavengers under aqueous conditions. Finally, we found the derivative that was the most efficient at radical scavenging in aqueous solutions was one that stabilized the active anionic form with an intramolecular base.

Acknowledgments

This work was supported in part by grants from the Health Science Foundation of the Ministry of Health, Labor, and Welfare of Japan.

Supplementary data

Supplementary data associated with this article can be found in the online version at doi:10.1016/j.bmcl.2006.09.005.

References and notes

1. Halliwell, B.; Gutteridge, J. M. *Methods Enzymol.* **1990**, *186*, 1.
2. Chapple, I. L. *J. Clin. Periodontol.* **1997**, *24*, 287.
3. von Zglinicki, T.; Burkle, A.; Kirkwood, T. B. *Exp. Gerontol.* **2001**, *36*, 1049.
4. Darley-Usmar, V.; Halliwell, B. *Pharm. Res.* **1996**, *13*, 649.
5. Kawai, H.; Nakai, H.; Suga, M.; Yuki, S.; Watanabe, T.; Saito, K. I. *J. Pharmacol. Exp. Ther.* **1997**, *281*, 921.
6. Watanabe, T.; Yuki, S.; Egawa, M.; Nishi, H. *J. Pharmacol. Exp. Ther.* **1994**, *268*, 1597.
7. Wu, T. W.; Zeng, L. H.; Wu, J.; Fung, K. P. *Life Sci.* **2002**, *71*, 2249.
8. Yamamoto, Y.; Kuwahara, T.; Watanabe, K.; Watanabe, K. *Redox Rep.* **1996**, *2*, 333.
9. Ono, S.; Okazaki, K.; Sakurai, M.; Inoue, Y. *J. Phys. Chem. A* **1997**, *101*, 3769.
10. Watanabe, K.; Morinaka, Y.; Iseki, K.; Watanabe, T.; Yuki, S.; Nishi, H. *Redox Rep.* **2003**, *8*, 151.
11. Ueda, J.; Saito, N.; Shimazu, Y.; Ozawa, T. *Arch. Biochem. Biophys.* **1996**, *333*, 377.
12. Ueda, J.; Takai, M.; Shimazu, Y.; Ozawa, T. *Arch. Biochem. Biophys.* **1998**, *357*, 231.
13. Watanabe, K.; Watanabe, K.; Hayase, T. *Jpn. Pharmacol. Ther.* **1997**, *25*, 1699.
14. Watanabe, K.; Watanabe, K.; Kuwahara, T.; Yamamoto, Y. *J. Jpn. Oil Chem. Soc.* **1997**, *46*, 797.

Available online at www.sciencedirect.com

ScienceDirect

Bioorganic & Medicinal Chemistry Letters

ELSEVIER

Bioorganic & Medicinal Chemistry Letters 17 (2007) 1451–1454

Novel membrane-localizing TEMPO derivatives for measurement of cellular oxidative stress at the cell membrane

Shizuka Ban, Hidehiko Nakagawa,* Takayoshi Suzuki and Naoki Miyata*

Graduate School of Pharmaceutical Sciences, Nagoya City University, 3-1 Tanabe-dori, Mizuho-ku, Nagoya, Aichi 467-8603, Japan

Received 22 August 2006; revised 30 October 2006; accepted 13 November 2006
Available online 16 November 2006

Abstract—Oxidative stress affecting lipid membranes is considered to be closely related to cardiovascular disease and brain ischemia. In this study, we designed and synthesized membrane-localizing TEMPO derivatives and demonstrated that one of these synthesized probes, compound **1**, localized and detected oxidative stress in the cell membrane in an endotoxic model of a mouse macrophage-like cell line. Compound **1** is therefore a potentially useful probe for evaluating oxidative stress at the cell membrane.

It is known that about 1% of the oxygen taken into our bodies by breathing is metabolized to reactive oxygen species (ROS). ROS are considered to play important roles, not only in inflammation as protective factors, but also in signal transduction.[1] On the other hand, it is also known that ROS react with lipids, proteins, sugars, and DNA, causing oxidative stress when produced in excess.[2] These reactions are suggested to be a major cause of a variety of diseases and oxidative stress caused by their reaction with lipids is considered to be closely related to cardiovascular disease[3] and brain ischemia.[4] It appears important to evaluate oxidative stress with respect to lipids in order to understand the pathological conditions underlying these kinds of diseases. However, there have been only a few attempts to measure the oxidative stress induced by ROS in specific cellular regions.[5] ROS can be measured indirectly by means of their reaction with stable radical compounds in the cell, through which the radical probes are readily reduced to non-radical species.[6]

Among these radical species, 2,2,6,6-tetramethylpiperidin-1-oxyl (TEMPO) can be reduced to 2,2,6,6-tetramethylpiperidin-1-ol under physiological conditions, that is, TEMPO converts to the non-radical form by reduction.[7] When ROS are upregulated and cells are in a relatively oxidative environment, cellular reduction will be downregulated. Electron spin resonance (ESR) measurement is a useful approach to detect radical species in biological systems. Using TEMPOL (4-hydroxyl-2,2,6,6-tetramethyl-piperidin-1-oxyl), a useful TEMPO derivative, oxidative stress can be measured by ESR spectrometry.

TEMPOL is easily introduced into cells, but due to its amphiphilic nature can easily exit from cells as well.[8] TEMPO derivatives which localize to a particular cellular region would be useful for measuring oxidative stress, including stress on the cell membrane, and TEMPO derivatives localizing to the lipid membrane would be advantageous.

For this purpose, the TEMPO derivatives would require a radical moiety for ESR detection, a fluorescent group for identifying its cellular distribution, and a functional group for localizing to the lipid membrane in a cell.

In this study, we designed and synthesized TEMPO derivatives with an alkyl chain for localization to the cell membrane (Fig. 1), and demonstrated that these radical probes were able to detect oxidative stress in lipid bilayers in an endotoxic model of a mouse macrophage-like cell line.

Mouse RAW264.7 cells were cultured in DMEM containing penicillin and streptomycin, supplemented with fetal bovine serum. For the experiments, the cells were plated onto 10-cm culture dishes at 1.5×10^7 cells/dish with 15 mL DMEM. The cells were incubated at 37 °C

Keywords: Fluorescein; Redox; Electron spin resonance; Reactive oxygen species; Superoxide; Inflammation.
* Corresponding authors. Tel.:/fax: +81 52 836 3407; e-mail addresses: deco@phar.nagoya-cu.ac.jp; miyata-n@phar.nagoya-cu.ac.jp

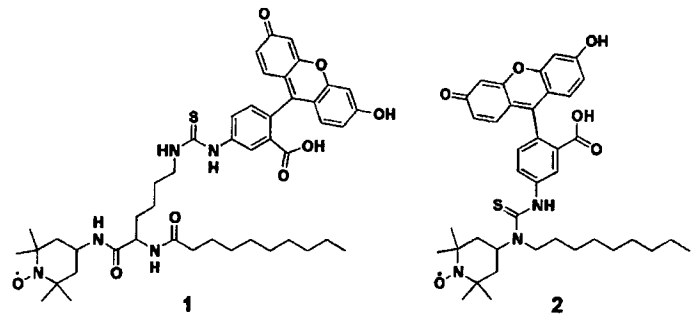

Figure 1. Structures of TEMPO derivatives designed to localize to cell membranes.

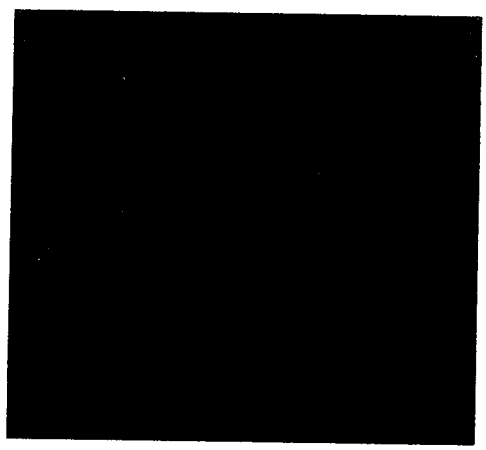

Figure 2. Distribution of 1 in RAW264.7 cells. The cells were stained with 1 (green) and Hoechst 33342 (blue), and then observed by confocal fluorescence microscopy.

in a humidified 5% (v/v) CO_2 incubator for 2 days. Then, the culture medium was replaced with 5 mL of serum-free DMEM, and the cells were treated with LPS (*E. coli*, 0.5 μg/mL) and IFN-γ (human recombinant, 150 U/mL). The treated cells were subsequently cultured for 5 h, washed 2 times with Dulbecco's PBS (D-PBS), and then treated with 100 μM of **1** for 10 min in dark. Following this, they were washed 3 times with D-PBS. The cells were then scraped into 2 mL D-PBS, and 1 mL of the cell suspension was used for ESR experiments.

Each suspension of treated cells was placed in a flat quartz cuvette. ESR measurements were started 15 min after the treatment with **1**. The ESR signal was recorded at 5-min intervals. The signal intensity (I) was calculated from the 2nd integral of the signal trace and expressed as a ratio (I/I_0) by comparing it to the intensity of the standard Mn^{2+} signal (I_0). The signal decay rate was calculated as the pseudo first order rate of the decrease in the ratio (I/I_0).

For confocal microscopy, the cells were plated on a 3-cm glass-bottomed culture dish at 1.5×10^5cells/dish with 1.5 mL DMEM, and incubated at 37 °C in a humidified 5% (v/v) CO_2 incubator for 2 days. The cells were treated with **1** or **2** in the same manner as for the ESR experi-

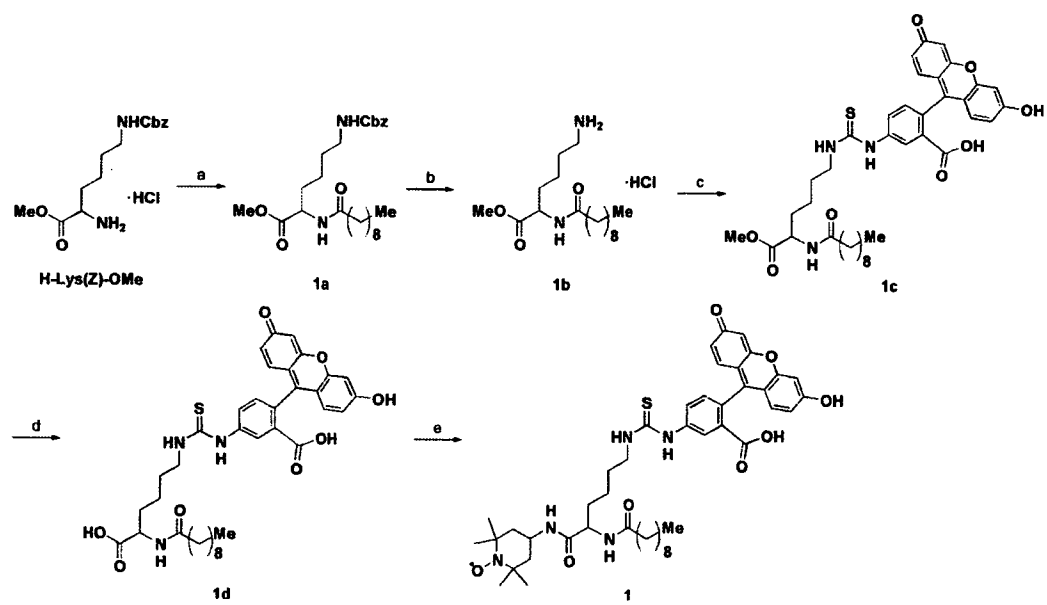

Scheme 1. Synthesis of compound 1. Reagents and conditions: (a) *n*-decanonyl chloride, Et_3N, CH_2Cl_2, 99%; (b) Pd–C, H_2, MeOH, then 4 N HCl/AcOEt, 88%; (c) FITC, Et_3N, EtOH, 51%; (d) LiOH aq, THF, EtOH, 98%; (e) 4-amino-TEMPO, EDCI, HOBt, DMF, 55%.

ments. The cells were subsequently stained with Hoechst 33342 for 10 min and subjected to confocal fluorescence microscopy.

The confocal microscopic study of the RAW264.7 cells treated with compound **1** indicated that **1** was localized to the cell membrane as expected (Fig. 2), due to the presence of its alkyl chain. The TEMPO moiety was assumed to be close to the surface in the lipid bilayer because the signal shape was not broad, as compared with the signal of TEMPOL in solution (Supporting information). This probe is considered to be able to penetrate into the lipid bilayer for its adequate lipid solubility. Compounds **1** and **2** are assumed to be distributed at the both leaflets of the cell membrane. Thus, the probe can measure the oxidative stress at the cell membrane (Scheme 1 and Scheme 2).

There are no differences in localization and sensitivity between compounds **1** and **2** in the observation by confocal fluorescence microscopy. Compound **1** was used for ESR analysis because it was more stable than compound **2** in solution. The ESR signal of **1** was measured in RAW264.7 cells to evaluate oxidative stress in the cell

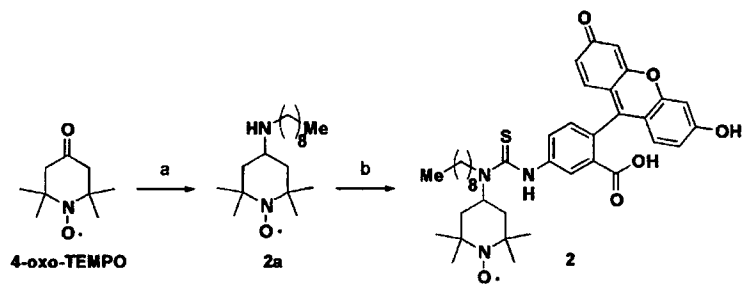

Scheme 2. Synthesis of compound **2**. Reagents and conditions: (a) *n*-nonylamine, THF, then $NaBH(OAc)_3$, 84%; (b) FITC, THF, 41%.

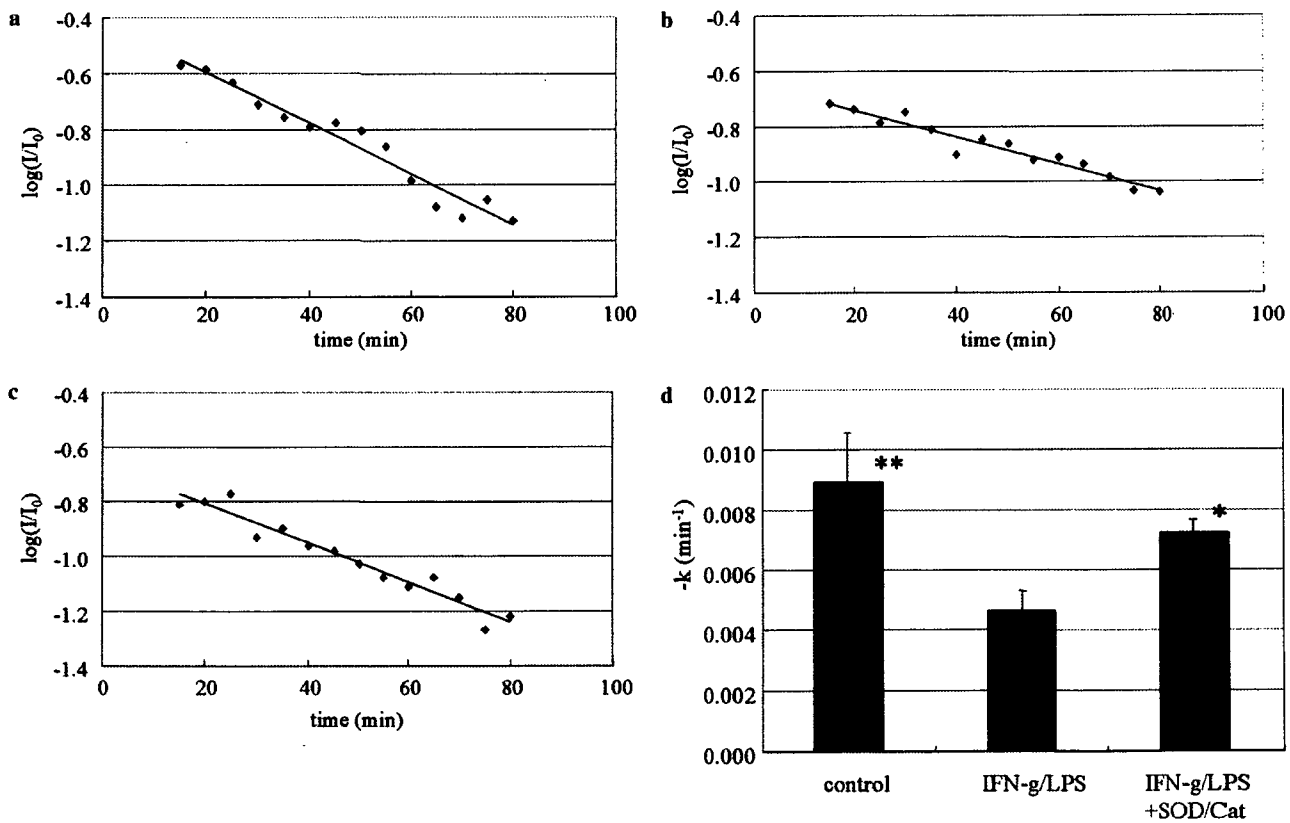

Figure 3. The time course of the relative signal intensity measured at 5-min intervals, (a) control cells, (b) LPS/IFN-γ-treated cells, and (c) LPS/IFN-γ-treated cells in the presence of SOD and catalase. I, compound **1** peak area; I_0, Mn^{2+} external standard peak area. (d) Signal decay rate of **1** in RAW264.7 cells. The signal decay rates of **1** with RAW264.7 cells were calculated from ESR signal intensities of **1** in RAW264.7 cells treated with vehicle, or with LPS/IFN-γ in the presence or absence of SOD/catalase. Values are presented as means ± SD of 3 or 4 experiments. ANOVA and Bonferroni-type multiple t-test indicated significant differences between LPS/IFN-γ and the control ($^{**}P < 0.01$), and LPS/IFN-γ + SOD/catalase ($^{*}P < 0.05$).

membrane. In the control cells, the signal intensity of **1** was gradually decreased at $0.0091 \pm 0.002\ min^{-1}$ under our conditions. The upregulation of oxidative stress was evaluated after endotoxic stimulation. ESR spectra of **1** were measured in RAW264.7 cells treated with 500 ng/mL LPS and 150 U/mL IFN-γ for 5 h. The rate of signal decay observed in cells treated with LPS/IFN-γ was decreased to $0.0049 \pm 0.0007\ min^{-1}$. The decreased rate as a result of the LPS/IFN-γ treatment was restored to $0.0072 \pm 0.0004\ min^{-1}$ in the presence of 100 U/mL SOD and 10 U/mL catalase during measurement (Fig. 3d). In the absence of the RAW264.7 cells, the signal failed to decay (data not shown).

Since cells generally exist in a reductive environment, compound **1** was found to be gradually reduced to the non-radical species in the presence of the control cells. Treatment with LPS/IFN-γ activated the cells and increased the production of reactive oxygen and nitrogen species (ROS/RNS). LPS/IFN-γ treatment also decreased the decay rate of nitroxyl radical. The decrease in this rate was recovered in the presence of 100 U/mL SOD and 10 U/mL catalase. Although ROS were still upregulated by LPS/IFN-γ treatment, they were considered to be at least partially scavenged by SOD and catalase. The probe was reduced under any conditions in our experiment, and the decay rate was considered to reflect the cellular local reducing ability for the probe, which would correlate with the oxidative stress in the cell membrane. Thus, the decay rate of **1** was not assumed to reflect specific ROS production, but the local oxidant upregulation, although the production of superoxide was upregulated under this experimental condition, and superoxide, hydrogen peroxide, and hydroxyl radical were considered to play an important role in this result. It was suggested that the cell membrane was exposed to an oxidative environment due to the increase in ROS by LPS/IFN-γ-pretreatment. Although SOD and catalase were thought not to be distributed inside the cells, they were able to get close to the cell membrane, where compound **1** was localized. These two enzymes may contribute to the scavenging of ROS around the cell membrane, and this is consistent with the fact that ESR signal decay rate was restored under these conditions. The change in this rate was assumed to be due to either a decrease in the cellular reductants by ROS upregulation or an increase in the oxidation of hydroxylamine, a reduced form of **1**.[9] The TEMPO moiety can be oxidized to the ESR-silent oxonium cation form by superoxide.[10] However, this cation was found to be rapidly reduced back to TEMPO by the superoxide itself.[10] Compound **1** was considered to be repeatedly oxidized and reduced in the cell membrane. The direct oxidation of TEMPO itself by superoxide probably does not affect the signal decay rate under the condition used for these measurements.

In conclusion, although there remain some detailed characteristics to be clarified, compound **1** was found to be a useful probe for evaluating oxidative stress at the cell membrane.

Supplementary data

Supplementary data associated with this article can be found, in the online version, at doi:10.1016/j.bmcl.2006.11.040.

References and notes

1. (a) Irani, K.; Goldschmidt-Clermont, P. J. *Biochem. Pharmacol.* **1998**, *55*, 1339; (b) Irani, K.; Xia, Y.; Zweier, J. L.; Sollott, S. J.; Der, C. J.; Fearon, E. R.; Sundaresan, M.; Finkel, T.; Goldschmidt-Clermont, P. J. *Science* **1997**, *275*, 1649.
2. Darley-Usmar, V.; Halliwell, B. *Pharm. Res* **1996**, *13*, 649.
3. (a) Ballinger, S. W. *Free Radic. Biol. Med.* **2005**, *38*, 1278; (b) Molavi, B.; Mehta, J. L. *Curr. Opin. Cardiol.* **2004**, *19*, 488.
4. (a) Love, S. *Brain Pathol.* **1999**, *9*, 119; (b) Sweeney, M. I.; Yager, J. Y.; Walz, W.; Juurlink, B. H. *Can. J. Physiol. Pharmacol.* **1995**, *75*, 1525.
5. (a) Wipf, P.; Xiao, J.; Jiang, J.; Belikova, NA.; Tyurin, V. A.; Fink, M. P.; Kagan, V. E. *J. Am. Chem. Soc.* **2005**, *127*, 12460; (b) Okamoto, A.; Inasaki, T.; Saito, I. *Bioorg. Med. Chem. Lett* **2004**, *14*, 3415; (c) Freedman, J. E.; Keaney, J. F., Jr. *Methods Enzymol.* **1999**, *301*, 61.
6. Nakagawa, H.; Moritake, T.; Tsuboi, K.; Ikota, N.; Ozawa, T. *FEBS Lett.* **2000**, *471*, 187.
7. (a) May, J. M.; Qu, Z. C.; Juliao, S.; Cobb, C. E. *Free Radic. Res.* **2005**, *39*, 195; (b) Samuni, A.; Goldstein, S.; Russo, A.; Mitchell, J. B.; Krishna, M. C.; Neta, P. *J. Am. Chem. Soc.* **2002**, *124*, 8719; (c) Iannone, A.; Bini, A.; Swartz, HM.; Tomasi, A.; Vannini, V. *Biochem. Pharmacol.* **1989**, *38*, 2581.
8. Cuzzocrea, S.; McDonald, M. C.; Mazzon, E.; Dugo, L.; Lepore, V.; Fonti, M. T.; Ciccolo, A.; Terranova, M. L.; Caputi, A. P.; Thiemerann, C. *Eur. J. Pharmacol.* **2000**, *406*, 127.
9. Zigler, J. S., Jr.; Qin, C.; Kamiya, T.; Krishna, MC.; Cheng, Q.; Tumminia, S.; Russell, P. *Free Radic. Biol. Med.* **2003**, *35*, 1194.
10. Krishna, MC.; Russo, A.; Mitchell, JB.; Goldstein, S.; Dafni, H.; Samuni, A. *J. Biol. Chem.* **1996**, *271*, 26026.

Available online at www.sciencedirect.com

ScienceDirect

Bioorganic & Medicinal Chemistry Letters

ELSEVIER

Bioorganic & Medicinal Chemistry Letters 17 (2007) 1558–1561

Identification of a potent and stable antiproliferative agent by the prodrug formation of a thiolate histone deacetylase inhibitor

Takayoshi Suzuki,[a,*] Shinya Hisakawa,[a] Yukihiro Itoh,[a] Sakiko Maruyama,[b] Mineko Kurotaki,[b] Hidehiko Nakagawa[a] and Naoki Miyata[a,*]

[a]*Graduate School of Pharmaceutical Sciences, Nagoya City University, 3-1 Tanabe-dori, Mizuho-ku, Nagoya, Aichi 467-8603, Japan*
[b]*Evaluation Group, Drug Research Department, R&D Division, Pharmaceuticals Group, Nippon Kayaku Co., Ltd, 31-12, Shimo 3-chome, Kita-ku, Tokyo 115-8588, Japan*

Received 29 November 2006; revised 22 December 2006; accepted 29 December 2006
Available online 13 January 2007

Abstract—To identify prodrugs of a thiolate histone deacetylase inhibitor NCH-31 that show potent antiproliferative activity and are stable in human plasma, we synthesized several candidate prodrugs of NCH-31. Among these compounds, *S*-2-methyl-3-phenylpropanoyl compound **2** showed more potent antiproliferative activity and higher stability in human plasma than *S*-isobutyryl compound NCH-51.

The dynamic homeostasis of the nuclear acetylation of histones is regulated by the opposing activity of the enzymes histone acetyl transferases and histone deacetylases (HDACs).[1,2] Deacetylation of histone lysine residues is associated with a condensed chromatin structure resulting in transcriptional repression, whereas acetylation of histones is associated with a more open chromatin configuration and activation of transcription.[3] Aberrant activation of HDACs results in the transcriptional repression of oncoprotein and is linked to the malignant phenotypes of tumors.[4,5] Inhibition of HDACs causes histone hyperacetylation which leads to the disruption of the chromatin structure and the transcriptional activation of genes associated with cancer.[3,6] In addition, it has recently been reported that inhibition of an HDAC exerts antitumor effects through the non-transcriptional pathway in addition to the intervention of transcriptional regulation.[7,8] Indeed, HDAC inhibitors such as trichostatin A (TSA) and suberoylanilide hydroxamic acid (SAHA) (Fig. 1) have potent anticancer effects in vitro and in vivo.[9,10]

In the course of our study of HDAC inhibitors, we found that a series of thiol-based analogues, including NCH-31 (Fig. 2), are potent HDAC inhibitors.[11] Thiols are thought to inhibit HDACs by coordinating the zinc ion in the active site which is required for deacetylation of the acetylated lysine substrate. Further, the *S*-isobutyryl prodrug NCH-51 (Fig. 2), which is thought to be hydrolyzed to free thiol within cells, showed antiproliferative activity against cancer cells,[12] however, NCH-51 has stability problems. NCH-51 was vulnerable to human plasma metabolism at the remaining rate of approximately 50% after 24 h of incubation. We therefore decided to search for prodrugs that are more stable in human plasma and exert more potent antiproliferative activity than NCH-51.

Since prodrugs with a less hindered acyl group tended to exhibit less potent antiproliferative activity,[12] we designed *S*-acyl prodrugs **1–4** which bear an acyl group more bulky than NCH-51. Four candidate prodrugs of NCH-31 were synthesized as shown in Scheme 1. The sulfhydryl group of NCH-31 was acylated with the corresponding carboxylic acid to give the desired compounds **1–4**.

The compounds synthesized in this study were initially tested in antiproliferative activity assays using human lung cancer NCI-H460 cells and human breast cancer MDA-MB-231 cells (Table 1).[13] Although *S*-2-methoxy-2-phenylacetyl compound **3** and 3-phenyl-2-(phenylmethyl)propanoyl compound **4** were less active than thiol NCH-31 and its *S*-isobutyryl prodrug NCH-51,

Keywords: Histone deacetylase inhibitor; Antiproliferative agent; Prodrug.
* Corresponding authors. Tel./fax: +81 52 836 3407 (N. M.); e-mail addresses: suzuki@phar.nagoya-cu.ac.jp; miyata-n@phar.nagoya-cu.ac.jp

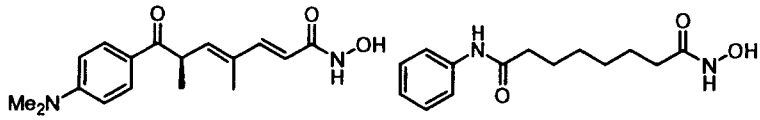

TSA SAHA

Figure 1. Structures of TSA and SAHA.

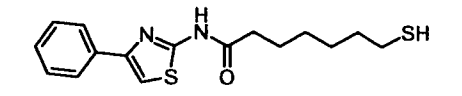

NCH-31

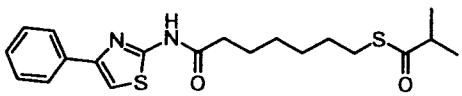

NCH-51

Figure 2. Structures of NCH-31 and NCH-51.

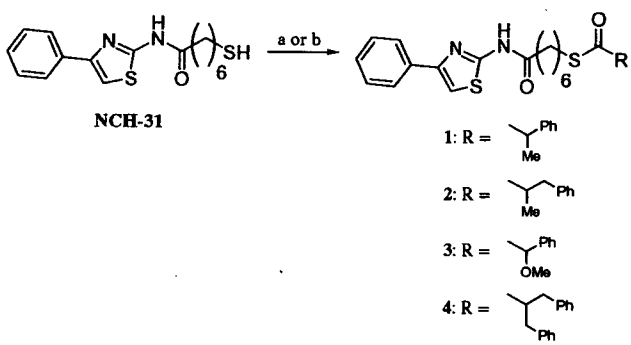

Scheme 1. Reagents and conditions: (a) RCOCl (for **1** and **4**), DMAP, pyridine, 0 °C to rt, 41% for **1**, 54% for **4**; (b) RCOOH (for **2** and **3**), EDCI, DMAP, DMF, rt, 63% for **2**, 23% for **3**.

S-2-phenylpropanoyl compound **1** showed similar activity against NCI-H460 cells and *S*-2-methyl-3-phenylpropanoyl compound **2** also displayed similar activity against both NCI-H460 cells and MDA-MB-231 cells when compared with NCH-51. Furthermore, we examined proliferation inhibition by NCH-51, compounds **1** and **2**, against eight solid cancer cell lines. As can be seen from Table 2, compound **2** showed potent proliferation inhibition against various cancer cells representing a 2-fold improvement over NCH-51 (average EC_{50} of **2** 2.4 μM, NCH-51 4.9 μM).

To investigate the difference in activity between (*R*)-**2** and (*S*)-**2**, optically active (*R*)-**2** and (*S*)-**2** were prepared from (*S*)-4,5,5-trimethyloxazolidin-2-one **5**[14] as outlined in Scheme 2. The chiral auxiliary **5** was converted to compounds **6** and **7** by *N*-propionylation and *N*-3-phenylpropionylation, respectively. Stereoselective enolate benzylation of **6** and methylation of **7**, and the subsequent hydrolysis of **8** and **9** gave optically active 2-methyl-3-phenylpropanoic acids (*R*)-**10** and (*S*)-**10**, respectively. The condensation of carboxylic acids

Table 1. Proliferation inhibition data on NCI-H460 cells and MDA-MB-231 cells for NCH-31, NCH-51, and compounds 1–4[a]

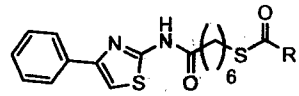

Compound	R	EC_{50} (μM)	
		NCI-H460	MDA-MB-231
NCH-31	–H	7.6	>20
NCH-51		2.1	4.4
1		3.2	>20
2	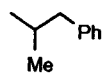	1.5	1.9
3		11	>20
4	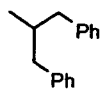	>20	>20

[a] Values are means of at least two experiments.

(*R*)-**10** and (*S*)-**10** with NCH-31 in the presence of EDCI and DMAP afforded optically active (*R*)-**2** and (*S*)-**2**, respectively. The enantiomeric excess of both (*R*)-**2** and (*S*)-**2** was determined to be 90% by chiral column chromatography.[15]

We examined the antiproliferative activity of (*R*)-**2** and (*S*)-**2** against four cancer cell lines, and there was not much difference between the activities of the two stereoisomers (Table 3).

Next, we investigated the in vitro HDAC inhibitory activity of compound **2** (Table 4).[16] Although NCH-31 exhibited potent inhibitory activity against HDAC1 (IC_{50} = 0.048 μM), the *S*-2-methyl-3-phenylpropanoyl prodrug **2** did not inhibit HDAC1 at a concentration of 100 μM.

Compound **2** was evaluated for the accumulation of acetylated histone H4 using Western blot analysis (Fig. 3).[17] Treatment of HCT116 cells with compound **2** produced an increase in the accumulation of acetylated histone H4, which indicated that the antiproliferative activity of compound **2** significantly correlates with the inhibition of HDACs. Since *S*-2-methyl-3-phenylpropanoyl prodrug **2** was totally inactive in an enzyme assay